

UNCLASSIFIED

AD NUMBER	
AD370910	
CLASSIFICATION CHANGES	
TO:	unclassified
FROM:	confidential
LIMITATION CHANGES	
TO: Approved for public release, distribution unlimited	
FROM: Distribution authorized to DoD only; Administrative/Operational Use; SEP 1965. Other requests shall be referred to Naval Radiological Defense Lab., San Francisco, CA.	
AUTHORITY	
CNR ltr, 5 May 1994; CNR ltr, 5 May 1994	

THIS PAGE IS UNCLASSIFIED

SECURITY

MARKING

The classified or limited status of this report applies to each page, unless otherwise marked.

Separate page printouts MUST be marked accordingly.

THIS DOCUMENT CONTAINS INFORMATION AFFECTING THE NATIONAL DEFENSE OF THE UNITED STATES WITHIN THE MEANING OF THE ESPIONAGE LAWS, TITLE 18, U.S.C., SECTIONS 793 AND 794. THE TRANSMISSION OR THE REVELATION OF ITS CONTENTS IN ANY MANNER TO AN UNAUTHORIZED PERSON IS PROHIBITED BY LAW.

NOTICE: When government or other drawings, specifications or other data are used for any purpose other than in connection with a definitely related government procurement operation, the U. S. Government thereby incurs no responsibility, nor any obligation whatsoever; and the fact that the Government may have formulated, furnished, or in any way supplied the said drawings, specifications, or other data is not to be regarded by implication or otherwise as in any manner licensing the holder or any other person or corporation, or conveying any rights or permission to manufacture, use or sell any patented invention that may in any way be related thereto.

CONFIDENTIAL

Copy No.

DASA 1726

USNRDL-TR-954

30 September 1965

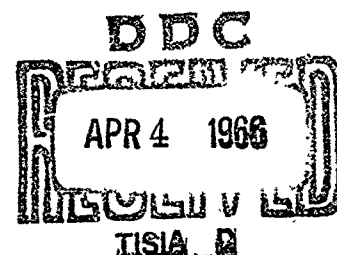
370910

HYDRA PROGRAM.

**HYDRA IIB SERIES - TRANSFER AND DISTRIBUTION OF
TRACED EXPLOSION PRODUCTS TO THE COLUMNS OF
SHALLOW UNDERWATER EXPLOSIONS (U)**

by

K. W. Kaulum



This document contains Restricted Data within the meaning of the Atomic Energy Act of 1954. Its transmission or the revelation of its contents in any manner not authorized by that Act is prohibited by law.

**U.S. NAVAL RADIOLOGICAL
DEFENSE LABORATORY**

SAN FRANCISCO • CALIFORNIA • 94135

GROUP-1
Excluded from automatic
downgrading and declassification.

FORMERLY RESTRICTED DATA

Handle as Restricted Data in Foreign Dissemination. Section 144b, Atomic Energy Act, 1954.

CONFIDENTIAL

RADIOLOGICAL EFFECTS BRANCH
E. A. Schuert, Head

CHEMICAL TECHNOLOGY DIVISION
R. Cole, Head

ADMINISTRATIVE INFORMATION

The work reported is part of a project sponsored by the Defense Atomic Support Agency under NWER Program A-7, Subtask 10.002f

ACKNOWLEDGMENT

The author wishes to acknowledge the efforts of all those people who participated in the rather lengthy and strenuous experimental work required to acquire the data included in this report. Their consistent attention to experimental details over a long period has contributed in large part to successful completion of the project.

Of these people, John R. Lai is due special mention because of his excellent handling of all radiochemistry for the project. His competence and foresight were responsible for making use of the radioactive tracer successful in every respect.

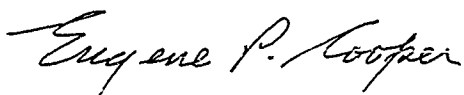
DDC AVAILABILITY NOTICE

U. S. Military Agencies may obtain copies of this report directly from DDC. Other qualified users should request through Director, DASA.

SECURITY


Reproduction of this document in any form by other than activities of the Department of Defense is not authorized unless specifically approved by the Secretary of the Navy or the Chief of Naval Operations as appropriate.

Extracts may be made from this document by activities of the Department of Defense when necessary for promulgation of information on defense against atomic warfare agents, or when necessary for inclusion in documents of the same or higher classification. Such extracts shall be classified, safeguarded and accounted for as set forth in the U. S. Navy Security Manual for Classified Matter.



Eugene P. Cooper
Scientific Director

12ND NRDL P5 (9/63)



D.C. Campbell, CAPT USN
Commanding Officer and Director

C O N F I D E N T I A L

ABSTRACT

The transfer of explosion products into the above-surface column and crown of a shallow underwater explosion was investigated with traced (Au^{198}) one-pound spherical pentolite charges fired at depths of 1.6 to 7.5 in. Tracer transfer data was obtained both by water sampling within the columns and radiation measurements adjacent to the columns. Radial tracer distributions in the column were integrated to give the total fraction of tracer transferred into the column as a function of time. A maximum of 5 % of the tracer was transferred into the column at the shallowest charge depth. Data analysis has established three distinct modes of tracer transfer into the above-surface columns or plumes which are shown to be associated with hydrodynamic processes involving the column or the explosion product bubble. The results are applied to full scale nuclear yields by utilizing a modified radial flow bubble model as a means of predicting the expected fission product transfer modes for specific nuclear yield and depth conditions.

This document contains information affecting the National Defense of the United States within the meaning of the Espionage Laws, Title 18, U. S. C., Section 793 and 794. Its transmission or the revelation of its contents in any manner to an unauthorized person is prohibited by law.

C O N F I D E N T I A L

C O N F I D E N T I A L

SUMMARY

PROBLEM

Accurate prediction of the above-surface radiological effects resulting from a shallow underwater nuclear explosion requires a complete knowledge of the mechanisms by which the fission products are transported from the explosion bubble to the surface environment. A complete phenomenology for shallow underwater explosions is not currently available; however, considerable progress has been made both theoretically and experimentally with high explosive in the area of hydrodynamics of the bubble and above-surface columns. This investigation is concerned with the explosion or fission product transfer mechanisms and their relation to the hydrodynamic processes of the bubble and columns.

FINDINGS

For small scale shallow underwater explosions, the traced explosion products were found to transfer into the column or plumes in three distinct modes or phases. Each of the transfer phases was related to a hydrodynamic process. Phase I is associated with the bubble top oscillation, phase II with the column walls, and phase III with the bubble bottom oscillation (late emission process).

C O N F I D E N T I A L

C O N F I D E N T I A L

A modified form of the radial flow bubble model which predicts the independent motions of bubble top and bottom for any yield can be employed as a means of predicting the expected modes of fission product transfer at nuclear yields.

Only a small fraction (approximately 5 %) of the traced explosion products were transferred into the column via phases I and II, at very shallow charge depths (in deep water); and virtually none at Umbrella scaled charge depths and deeper.

C O N F I D E N T I A L

PREFACE

This Laboratory has conducted the HYDRA Program in order to determine the radiological effects from underwater nuclear explosions. The ultimate objective was to analyze and express as functions of yield and depth of burst those radiological effects that can influence fleet and aircraft operations and/or design. The Program included a series of field tests to investigate comparable nuclear phenomena through the use of high explosive charges. This project, Hydra IIB, includes several of the test series in the program, in which the experimentation was limited to shallow underwater explosions of 1-pound charges.

Hydra IIB consisted of several experimental phases: (1) determination of the water motion adjacent to the expanding underwater bubble; (2) determination of the dynamic internal structure of the above surface column; (3) determination of the transfer mechanism of explosion products from the underwater bubble into the column and their distribution within the column. The first two phases are reported in References 1 and 2. The subject of this report is the third phase along with application of the results of all three phases to high-yield nuclear detonations.

Results of the Hydra Program currently are being utilized to compute the radiation fields from shallow underwater nuclear detonations. These computations require a knowledge of the distribution and mechanisms of release of fission products in the above-surface columns. Since almost no information of this kind has resulted from weapons tests,

C O N F I D E N T I A L

C O N F I D E N T I A L

investigators have been forced to assume distributions. The transfer mechanisms and fission product distributions described in this report should be applicable to these computations.

v

C O N F I D E N T I A L

C O N F I D E N T I A L

CONTENTS

ABSTRACT.	1
SUMMARY	ii
PREFACE	iv
INTRODUCTION.	1
Background	2
Objectives	4
Approach	5
EXPERIMENTAL DETAILS.	7
Test Facilities.	7
Explosive Charges and Tracer	8
Instrumentation.	11
Procedure.	15
Charge and Tracer Handling.	19
Sampler Set-Up.	20
Sample Treatment.	21
RESULTS.	22
Tracer Distribution.	22
Total Tracer in Column	23
Water Distribution in the Column	32
Gamma Radiation Adjacent to the Column	33
ANALYSIS AND DISCUSSION.	38
Transfer and Distribution of Tracer by Sampling.	38
Gamma Radiation Adjacent to the Column.	41
Transfer Mechanisms of Explosion Product Tracer into the Column.	44
Application of Results to Nuclear Phenomena	55
Shallow Bottom Effects.	62
CONCLUSIONS.	65
REFERENCES	67

C O N F I D E N T I A L

APPENDIX A	RADIAL DISTRIBUTIONS OF CUMULATIVE WATER SAMPLE VOLUME AND TOTAL EJECTED WATER VOLUME.	69
APPENDIX B	GAMMA DETECTOR COUNT RATE (100 msec interval) ADJACENT TO THE COLUMN FOR CHARGE DEPTHS OF 2.5, 3.5, 5.5, 7.5 AND 12 IN.	76
APPENDIX C	NUMBER OF COUNTS FROM THE GAMMA DETECTOR DURING THE FIRST 20 MSEC VS. DETECTOR HEIGHT FOR CHARGE DEPTHS OF 1.6 AND 3.5 IN.	79
APPENDIX D	HIGH RESOLUTION INITIAL COUNT RATE AT VARIOUS GAMMA DETECTOR HEIGHTS VS. TIME FOR CHARGE DEPTHS 1.6 TO 7.5 IN.	81
TABLES		
2.1	Summary of Shot Conditions (No. of Shots).	18
3.1	Fraction of Tracer in Column (%).	28
A.1	Charge Depth = 1.6 in.	70
A.2	Charge Depth = 2.5 in.	71
A.3	Charge Depth = 3.5 in.	72
A.4	Charge Depth = 5.5 in.	73
A.5	Charge Depth = 7.5 in.	74
A.6	Total Ejected Water (liters)	75
FIGURES		
2.1	General View of the Test Pond and Instrumentation- Support Structure.	9
2.2	Sampler Beam in Position with Samplers Instal.	9
2.3	Spherical Explosive Charge Designed for Tracer Insertion . . .10	
2.4	Details of Sampler.	12
2.5	Collimated Gamma Detector Assembly.	14
2.6	Off-Axis Response for Collimated Gamma Detector	16
3.1	A & B Sample Count Rate Per Millicurie of Tracer vs. Column Radius for 1.6 in. Charge Depth.	24
3.2	A & B Sample Count Rate Per Millicurie of Tracer vs. Column Radius for 2.5-in. Charge Depth.	25
3.3	A & B Sample Count Rate Per Millicurie of Tracer vs. Column Radius for 3.5 in. Charge Depth.	26
3.4	Total Fraction of Tracer in Column vs. Charge Depth for Nominal Sampling Height of 6 or 8 ft	29
3.5	Total Fraction of Tracer in the Column vs. Time for 2.5-in. Charge Depth.	30
3.6	Post-Shot Fraction of Tracer in the Pond vs. Charge Depth.	31
3.7	Gamma Count Rate (per 100-msec interval) vs. Time for 1.6-in. Charge Depth	34

C O N F I D E N T I A L

FIGURES (Cont'd)

3.8	Number of Counts During the First 20 msec vs. Detector Height Above Surface, for 2.5-in. Charge Depth.	36
3.9	High Time-Resolution Count Rate vs. Time for Initial 200-msec Period, at 2.5-in. Charge Depth.	37
4.1	Tracer Location Within Column During the Initial Excursion Period for Charge Depths 1.6, 2.5 and 5.5 in.	45
4.2	Predicted Bubble Top Half-Period vs. Charge Depth, with Tracer Reversal Times at Standard Charge Depths. . . .	47
4.3	Schematic Illustrations of Explosion Product Transfer and Related Hydrodynamic Processes for Charge Depth 2.5 in.	49
4.4	Calculated Ratio of Bubble Top Period to Bubble Bottom Period vs. Scaled Depth for 1 lb, 10^4 lb and 10 KT yields.	57
4.5	Initial Gamma Pulse From 1 lb, 10^4 lb and Nuclear Yields Time-Scaled With Calculated Bubble-Top Period . . .	59
B.1	Gamma Detector Count Rate (100 msec interval) Adjacent to the Column for Charge Depth of 2.5 in.	77
B.2	Gamma Detector Count Rate (100 msec interval) Adjacent to the Column for Charge Depth of 3.5 in.	77
B.3	Gamma Detector Count Rate (100 msec interval) Adjacent to the Column for Charge Depth of 5.5 in.	78
B.4	Gamma Detector Count Rate (100 msec interval) Adjacent to the Column for Charge Depth of 7.5 in.	78
B.5	Gamma Detector Count Rate (100 msec interval) Adjacent to the Column for Charge Depth of 12 in.	78
C.1	Number of Counts From the Gamma Detector During the First 20 msec vs. Detector Height for Charge Depth of 1.6 in. . .	80
C.2	Number of Counts From the Gamma Detector During the First 20 msec vs. Detector Height for Charge Depth of 3.5 in. . .	80
D.1	Data for each Detector Height at 2.5 in. Charge Depth . . .	83
D.2	High Resolution Initial Count Rate at Various Gamma Detector Heights vs. Time for Charge Depth 1.6 in.	85
D.3	High Resolution Initial Count Rate at Various Gamma Detector Heights vs. Time for Charge Depth 3.5 in.	86
D.4	High Resolution Initial Count Rate at Various Gamma Detector Heights vs. Time for Charge Depth 5.5 in.	87
D.5	High Resolution Initial Count Rate at Various Gamma Detector Heights vs. Time for Charge Depth 7.5 in.	88

C O N F I D E N T I A L

INTRODUCTION

Very little investigation has been made of the specific processes by which fission products are transferred from the underwater bubble into the column of a shallow underwater nuclear detonation. Radiological measurements made during weapons tests indicate only gross results, which yield little insight into these processes. Intelligent extension of these gross radiological measurements on a limited number of nuclear tests to other depths and yields requires a basic understanding of the transfer processes.

Precise understanding of these transfer processes requires that experimental work be accomplished at a scale that allows measurements to be made readily and multiple tests performed. Such experimentation can be done with one-pound high explosive charges and a radioactive tracer which satisfactorily simulate shallow nuclear detonations. Transfer mechanisms and distribution may then be investigated by physical sampling of the column and by above-surface measurement of radiation from the column.

Before proceeding further, it must be made clear that this study is mainly concerned with shallow underwater detonations, which are characterized by high above-surface columns, rather than deep detonations, where low bushy plumes result. Generally, shallow detonations are subdivided into "very shallow" and "shallow" scaled depths.⁹ The very shallow detonation produces a short cylindrical column topped by a crown, while the shallow detonation results in a high column with no

C O N F I D E N T I A L

C O N F I D E N T I A L

crown. Examples of each in the nuclear yield range are Crossroads Baker and Umbrella, respectively. These detonation depth classifications do not take the bottom depth into consideration.

BACKGROUND

The distribution and quantities of fission products in the columns of underwater nuclear detonations and the transfer mechanisms involved have been considered by only a few investigators in analyzing radiological effects data. Strobe's analysis³ of the total dose on the surface resulting from the Crossroads-Baker nuclear event indicated that a considerable fraction of the fission products had been transferred into the crown of the column, as evidenced by a ring of higher dose readings attributed to fallout. This conclusion has been controversial because only total dose data was considered. Also, no attempt was made to fix the total fraction of fission products in the crown.

Evans, in his analysis of the Umbrella radiological data,⁴ made little or no attempt to suggest either the fraction of fission products transferred into the column or possible transfer mechanisms. However, he did observe an initial gamma radiation pulse and concluded that its explanation required "some physical action which accomplishes the temporary submergence of the principal radiating source below the ocean surface," thus implying containment of fission products within the column.

Gross fallout from very shallow (Baker scale), high explosive, chemically traced shots was investigated with the HEM 1 and 3 field test series.⁵ Integration of the resulting surface fallout patterns from the columns showed that only about 20 % of the chemical tracer had been deposited. This would imply that even for very shallow detonation depths on or near the bottom, only a small fraction of the explosion products had been transferred into the columns. It should be noted that both this series and the

C O N F I D E N T I A L

Baker nuclear shot were detonated near shallow bottoms, which reasonably would be expected to influence the explosion product transfer into the column.

An intense study of radiological effects from underwater explosions using high explosives was started with the Hydra Program. In the Hydra I project,⁶ a radioactive tracer was introduced into 1-pound charges and the column was sampled at low heights. Although the Hydra I project provided a most extensive and useful documentation of shallow low-yield explosion phenomena, the sampling technique and conditions were insufficient to define the internal column structure and the explosion product transfer mechanisms.

The Hydra IIA project⁷ employed a radioactive tracer in 10,000-pound high explosive charges to simulate very shallow and shallow nuclear underwater detonations. Gamma radiation fields were measured both at the surface and from dropsondes falling adjacent to the column in an attempt to determine the fraction of tracer within the upper portion of the column and crown. An initial radiation pulse similar to that seen by Evans for the Umbrella shot was observed in the surface radiation data. Also, the dropsonde data indicated that some tracer was transferred into the upper portion of the column for shallow-scaled depths.

The Hydra IIB series of experiments was established with the overall objective of understanding the hydrodynamic processes of underwater bubble and above-surface column development, and then determining the mechanism by which the explosion products are transferred into the column. The first phase of experimental work determined the flow of water adjacent to the expanding bubble and into the column by photographically tracking fluorescent dyes. Its objective was to evaluate the radial flow assumption used by Hammond's bubble model.⁸ The results are analyzed in Ref. 2. They show the flow not to be radial and potential functions are suggested

C O N F I D E N T I A L

to describe the flow paths for a more comprehensive bubble model. To avoid this complication, a revision of the bubble model in Ref. 8 is presented which takes advantage of the fact that only radial flow can occur along the vertical axis of symmetry where there is no tangential component. This simplified model predicts bubble top and bottom periods for a large range of yields and depths. The ratio of bubble top and bottom periods is suggested as a characteristic parameter of bubble motion.

The second experimental phase of the Hydra IIB series¹ utilized column sampling techniques at several heights to determine the dynamic internal structure of a shallow underwater explosion column. The internal structure was found to consist of upward flowing column walls during early bubble expansion, followed by convergence of the walls into a central jet which rises high into the air and a downward jet which penetrates through the underwater bubble.

OBJECTIVES

With the bubble motion and the dynamic structure of the column reasonably well understood for one-pound yields, it was possible to undertake the present study of explosion product transfer processes into the columns and crowns at very shallow and shallow scaled depths. In addition, these results were to be analyzed and compared with those from traced large-yield high explosive and nuclear events so as to extend understanding of such comparable processes.

Investigation of the explosion product transfer processes was accomplished through the following specific experimental objectives:

1. Determination of the explosion product tracer distribution with time in the column at several heights during the event.

C O N F I D E N T I A L

C O N F I D E N T I A L

2. Determination of the total fraction of tracer transferred into the column as a function of time.

3. Measurement of the gamma radiation adjacent to the column at several heights to determine the tracer location and distribution within the column.

APPROACH

The distribution of traced explosion products transferred to the column and crown was determined by water sampling of the column. Facilities and instrumentation for column sampling were the same as those used for the second phase experimental work concerned only with the column internal structure. The radioactive explosion product tracer contained in the water was of major interest during this experimental phase. Water samples were collected at two heights in the column by means of a series of samplers arranged across its diameter which could be closed at desired times. Multiple shots at each depth were used to vary sampling height and time. The quantity of tracer in the water samples was determined by standard counting procedures.

The explosion products were traced with a liquid radioactive tracer placed in a spherical shell near the center of a special spherical charge. The central location of the tracer within the charge was necessary to simulate the probable fission product distribution for nuclear explosions.^{9,10} The radial tracer distributions derived from sampling data were then integrated for the column, to give the total fraction of tracer in the column for the heights and times of sampling.

In addition, a very narrowly collimated radiation detector was used to help determine the precise location of the radioactive tracer within the column. The detector was located adjacent to the column, directed

C O N F I D E N T I A L

at its axis and positioned at various heights for each shot. The radiation data provided both a rough indication of the tracer location during the event and with more careful analysis, a means of following the tracer during the initial bubble expansion period.

Scaled charge depths of interest are in the "very shallow" and "shallow" depth classifications as defined in Ref. 9. Nuclear events Baker and Umbrella are approximately scaled by the depths 2.5 and 5.5 in. respectively. The actual depth range used was from 1.6 in. (~ 1 charge radius) to 12 in.; the specific depths being the same as have been used previously with similar charges. The test pond is sufficiently deep so that deep water firing conditions could be assumed.

C O N F I D E N T I A L

C O N F I D E N T I A L

EXPERIMENTAL DETAILS

TEST FACILITIES

This test series was conducted at the NRDL test-pond facility located at Camp Parks. The facility consists of a fresh water pond with its associated filter system, a movable instrumentation-support structure, a portable house used as a work shop and office, and an instrumentation van. A general view of the facility is shown in Fig. 2.1.

The pond has the shape of an 18-ft radius hemisphere with a 6-ft wide underwater camera bay extending 10 ft to the south. The pond is constructed of a 12-in.-thick reinforced concrete shell which will withstand detonation of 1-lb HE charges underwater to a depth of approximately 6 ft. The pond contains 90,000 gallons of fresh water at normal operating level. The water is continuously filtered through a 3-unit sand-bed fixed-filter system with a capacity of 100 gpm. When rapid removal of explosion products is desired, an additional diatomaceous-earth filter system with a capacity of 400 gpm is used as well.

The instrument-support structure provides for rigid positioning of instruments over the water surface at any height up to 12 ft. The fabricated steel structure spans the pond and is supported on wheels, facilitating movement away from the pond. A 12 x 12-ft frame within the upright rails can be raised by electric hoists to any height up to 12 ft above the water level and securely locked in place with pins at

C O N F I D E N T I A L

C O N F I D E N T I A L

6-in. intervals. This frame supports the sampler beam over the center of the pond in a north-south orientation. The streamlined sampler beam supports 15 complete sampling devices. It also protects the sampling devices and their associated wiring from the high-velocity water of the plume. Figure 2.2 shows the sampler beam in place with its cover open and the samplers installed.

EXPLOSIVE CHARGES AND TRACER

The explosive charges used were 1-pound, spherical pentolite charges drilled to receive a detonator and tracer at the center. The detonator is spherical, $5/8$ in. in diameter. It is surrounded by an absorbent paper shell $1/16$ in. thick, which will absorb approximately 1 ml of tracer solution. A pentolite plug closes the opening. Details of construction are shown in Fig. 2.3. The charges were electrically detonated by the thyatron-controlled discharge of a 20- μ fd capacitor charged to 1800 volts.

The charges were supported in firing position by a Lucite ring with a diameter smaller than that of the charge, and were held on the ring with a single wrap of electrical tape. The ring was supported by cords to a horizontal tension system. Both are seen below the sampler beam in Fig. 2.2.

The radioactive tracer Au^{198} was selected according to several requirements:

1. Short half-life (65 hr) to prevent excess build-up of pond water background.
2. High concentration (mc/ml), since the volume available in the charge is only 1 ml.
3. Gamma energy (0.411 Mev) suitable for high efficiency counting.

C O N F I D E N T I A L

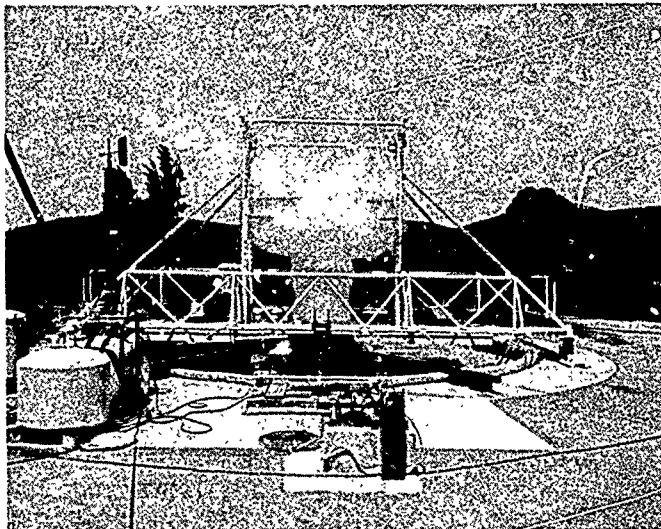


Fig. 2.1 General View of the Test Pond and Instrumentation-Support Structure. A shot is in progress.

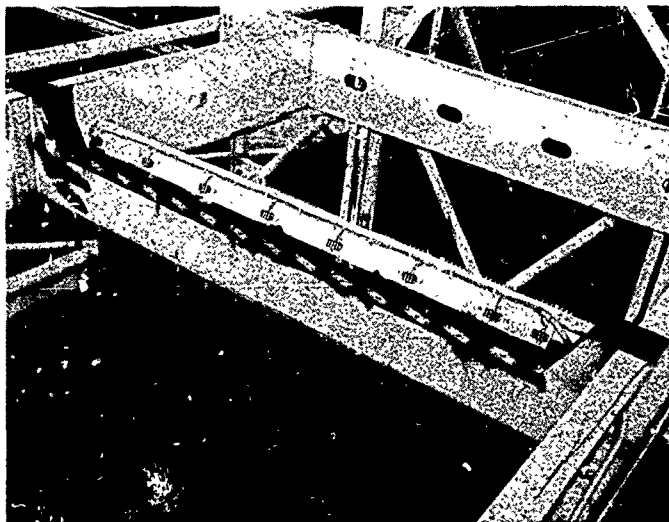


Fig. 2.2 Sampler Beam in Position with Samplers Installed

C O N F I D E N T I A L

C O N F I D E N T I A L

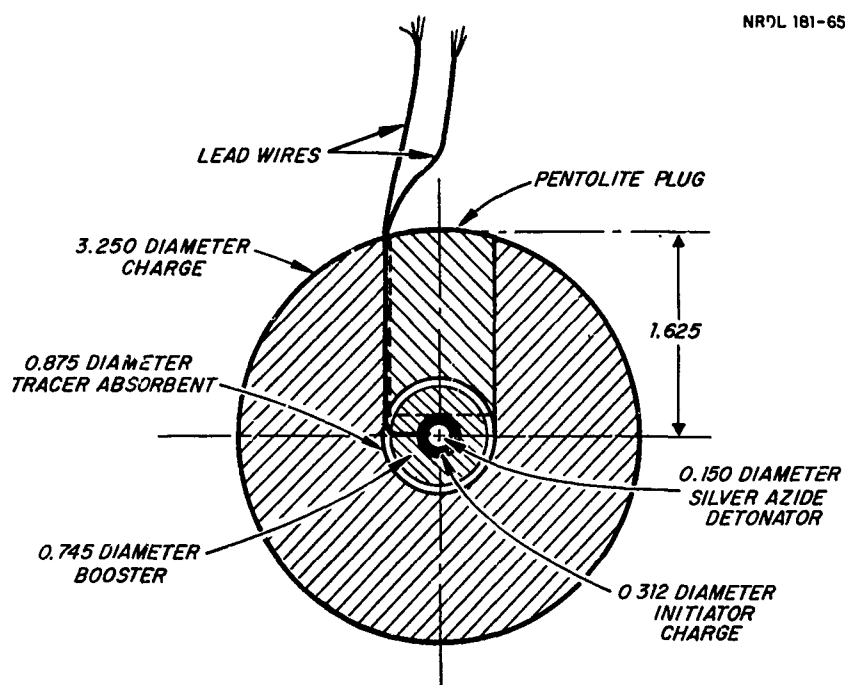


Fig. 2.3 Spherical Explosive Charge Designed for Tracer Insertion

C O N F I D E N T I A L

C O N F I D E N T I A L

Also, it is available at a nominal cost from Oak Ridge National Laboratory in the form of AuCl_3 dissolved in 1 N HCl solution.

I N S T R U M E N T A T I O N

Each sampler consists of a snout through which the water enters, a normally-open valve, and a sample reservoir. It has a straight 3/4-in. bore through to the reservoir cap, where the water impinges on a cone and is directed into the annular reservoir. The reservoir cap also has ten 1/4-in. vent holes to release any pressure build-up within the reservoir. Figure 2.4 is a sectional view of the entire sampler.

Because the sampler snout extends below the sampler valve, the normally-open valve is single-stage so that sampling is continuous until terminated by closure of the valve. This arrangement insures that the water sample does not include water retained in the snout from an earlier time as would be the case for a normally closed valve opened during the event. This cumulative arrangement requires, to obtain a sample volume for a specific interval of time, that volumes from successive shots with different termination times be subtracted from each other. The same sampler was used to obtain total event samples simply by not closing the valve during the event.

The sampler reservoir has a total volume of 450 ml; however, calibration tests have shown that total samples should be limited to 150 ml. When a total sample exceeding 150 ml was expected, the effective sampling area was reduced by a factor of five with a 3/8-in. bore orifice plug inserted into the end of the standard 3/4-in. diameter bore snout.

The sampler had been calibrated in a high-velocity spray of known bulk density to determine its effective sampling area and the effect of

C O N F I D E N T I A L

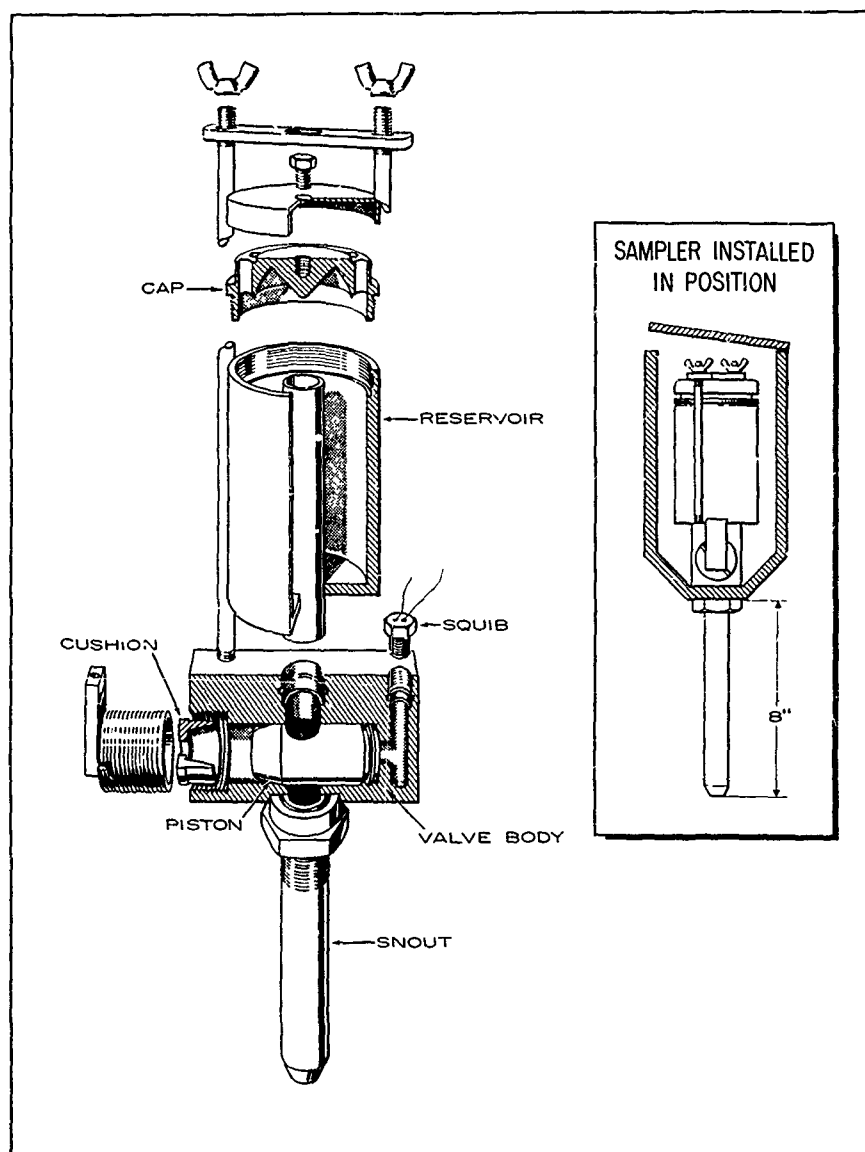


Fig. 2.4 Details of Sampler

C O N F I D E N T I A L

C O N F I D E N T I A L

non-axial sample approach. The details of this calibration are given in Ref. 1. The sampler reservoir and its cap were Teflon-coated so as to allow simple decontamination when the samplers were used for several shots in one day.

The valve section of the sampler was required to block flow into the reservoir at a precise, predetermined time during the event. This is accomplished by moving the piston along its horizontal axis to the closed position. The piston is actuated by an electrically initiated squib, or gas generator, and stopped at the end of its travel by a tapered brass cushion which absorbs the energy of the piston by a small radial deformation. The closing time of the valve is 1.1 msec or less. Calibration and performance of the valve are more fully described in Ref. 1.

The timing system for valve firing provides triggering voltages to the valve squibs at precise, ordered time intervals after shot zero time. Five separate valve-actuation times, each ranging from 0 to 900 msec, were available. However, the same time was normally selected for all samplers. Briefly, the system consists of an electronic counter-time unit with the output of 4 decades switched into diode logic units. The outputs of the logic units trigger thyratrons that allow capacitors to discharge through the squibs. A 10-channel event-programmer provides contact closures for starting cameras, recorders, and finally the counter-timer for the precision timing system.

The collimated gamma detector consists of a 2-1/4-in. diameter by 2-1/2-in. sodium iodide (thallium activated) crystal and a photomultiplier tube, mounted in a cylindrical lead collimator. This assembly weighed approximately 200 lb and could be positioned with relative ease. It was positioned 7 ft from the column axis at any desired height above the water surface up to 12 ft. It was mounted level and aimed at the column axis. A cross-section of this assembly is shown in Fig. 2.5.

C O N F I D E N T I A L

C O N F I D E N T I A L

NRDL 621-65

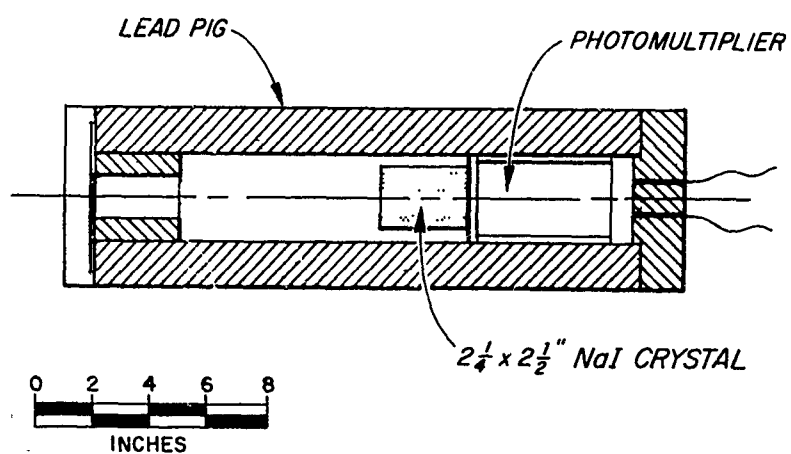


Fig. 2.5 Collimated Gamma Detector Assembly

C O N F I D E N T I A L

C O N F I D E N T I A L

The electronics associated with the detector were located in the instrument trailer, except for a small photomultiplier output cathode follower unit located on the collimator. The electronic system consisted of a high voltage supply for the photomultiplier tube, a cathode follower, a linear pulse amplifier, two Tektronix #535 oscilloscopes used as energy discriminators, and a high-speed oscillograph.

In order to reduce the background radiation seen by the system, an energy window was formed around the tracer's 0.4 Mev gamma energy. The two oscilloscopes were used as energy discriminators with one passing only pulses with an energy of 0.2 Mev or more and the other passing pulses with an energy of at least 0.8 Mev. The difference in the number of pulses from each channel then gave the resulting pulses between 0.2 and 0.8 Mev. Use of the oscilloscopes as discriminators was accomplished by feeding the output of the linear pulse amplifier into both oscilloscopes and adjusting their triggering levels appropriately, so as to trigger their horizontal sweep. Pulses from the oscilloscope sweep output then were recorded directly on separate channels of the high-speed oscillograph. A sweep time of 20 μ sec was used which allowed a maximum pulse rate of 50 K per second.

The collimator effectiveness was determined by locating a small Au¹⁹⁸ source successively in positions off the collimator axis and recording the resulting count rates. The response (relative to on-axis) drops off almost linearly with the off-axis position of the source at a 7 ft, 2 in. standoff, and reaches background level at 12 in. \pm 1 in. The response curve is shown in Fig. 2.6.

PROCEDURE

At the beginning of the experimental work, determination of the tracer distribution by sampling of the column was considered the most

C O N F I D E N T I A L

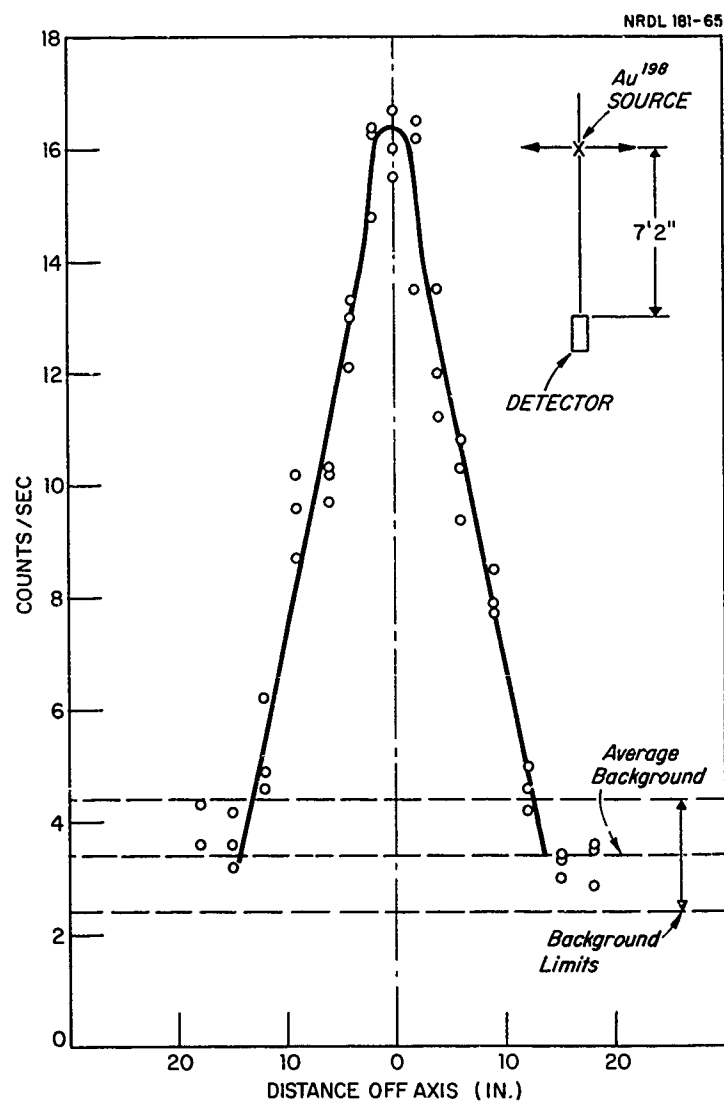


Fig. 2.6 Off-Axis Response for Collimated Gamma Detector

C O N F I D E N T I A L

C O N F I D E N T I A L

important means of accomplishing the objectives. The previous work on structure of the column had shown that convergence occurred at approximately 6 ft above the water surface for a charge depth of 5.5 in.; so that this was the minimum sampling height if sampling inside the bubble was to be avoided. This was necessary because the sampler is not suitable for sampling of gas. Also the approximate center of the column crown for the very shallow charge depths occurs at approximately 11 ft; so this upper height limit was selected.

An exploratory approach was used to choose charge depths and sampling conditions. Work was begun at a mid-range depth and nominal 6 ft sampling height, with sampling termination at late times. When little tracer was encountered, sampling of further shots was not continued to higher levels and shorter times, but rather a new series of shots at a shallower depth was begun. As more tracer was encountered at the shallower charge depth, higher sampling height and shorter termination times were selected to obtain a rough tracer distribution. This process resulted in a final selection of 8 and 11 ft nominal sampling heights for the 1.6 and 2.5 in. depths, 6 and 11 ft heights for the 3.5 in. depth, and only a 6 ft height for the 5.5, 7.5, and 12 in. depths. Final sampling times were 27, 52, 100 and 300 msec, and the duration of the total event. Table 2.1 gives a summary of the number of shots fired under each sampling condition.

Also included in this table are the number of shots for intervals of height at which gamma detector measurements were made. Here there are five detector height increments of 2 ft starting at less than 2 ft and extending up to 12 ft. Generally a gamma detector measurement was obtained for most sampling shots, but no shots were fired only for gamma detector measurements. The gamma detector was always mounted at a height lower than the samplers, so as to avoid measurements in a section of the column possibly disturbed by the sampling beam.

C O N F I D E N T I A L

TABLE 2.1
Summary of Shot Conditions
(No. of Shots)

Charge Depth (in.)	Nominal Sampling Height (ft)	Sampling Termination Time (msec)					Gamma Detector Height				
		27	52	100	300	Total Event	< 2 ft	2-4 ft	4-6 ft	6-8 ft	8-12 ft
1.6	8	1	2	1	4	-					
1.6	11	-	-	3	-	1	2	2	4	2	2
2.5	6	-	-	2	-	-					
2.5	8	2	2	3	3	1	4	5	6	2	4
2.5	11	2	2	2	1	-					
3.5	6	-	1	3	4	-					
3.5	11	-	-	2	2	-	1	3	3	3	1
5.5	6	-	2	2	2	-	1	1	-	1	-
7.5	6	-	-	1	1	-	-	1	-	1	-
12	6	-	-	1	1	-	-	3	-	-	-

C O N F I D E N T I A L

Charge and Tracer Handling

As indicated previously the radioactive tracer was inserted into the charge in the form of a solution. An air shipment of radioactive tracer was received weekly from Oak Ridge National Laboratory. This contained approximately 60 millicuries of activity in 0.1 to 0.4 ml of solution at the time of arrival. Pre-shot preparation of the tracer solution required only dilution of the solution, in the screw-top shipping bottle, to a total volume of approximately 2 ml. Although one ml of solution, containing approximately 20 millicuries, was used for a shot, two shots generally were fired in one day. Upon dilution the tracer solution was ready for transfer to the charge.

The first several shipments of tracer were assayed by standard counting techniques on a 25-λ sample, drawn with a micropipette, to check the declared quantity of radioactivity. These assays showed good agreement with the stated quantity; so that subsequently only every fourth shipment was assayed. It is estimated that the amount of activity delivered into the charge was known within $\pm 5\%$.

The explosive charge was prepared by assembling the absorbent shell around the detonator and installing them in the well. It was then mounted on the lucite ring, supported by the horizontal tension system several feet above the water surface, and precisely positioned on a vertical axis through the center sampler. Next the tracer solution was pipetted directly from the shipping bottle onto the absorbent shell within the charge. The plug of explosive material was inserted and sealed with a patch of electrical tape.

The charge support system was arranged so that the charge could be lowered without dislocation from the vertical axis. The charge depth was set by lowering until the charge top was just breaking the water

C O N F I D E N T I A L

surface. Then the lowering continued to the desired depth minus one charge radius, as indicated by the length of cable payed out. This method gives a charge depth accuracy of approximately $\pm 1/8$ in.

Sampler Set-Up

Before every shot, the sampler reservoirs were decontaminated by rinsing with fresh water. Tests had indicated that this procedure was sufficient to prevent cross-contamination between shots. Each sampler valve was reset to the open position and a new squib was installed, so that the sampler was ready for the next firing. The samplers were routinely overhauled, including replacement of the piston cushion, after every ten shots or when it became difficult to reset the piston to the open position.

Confidence in the reliability and accuracy of the sampling valve performance had been established during previous sampling experiments. On the assumption that valve performance did not vary, only the valve-firing system performance was checked by recording the valve-firing signals, along with the zero time of each shot, on the oscillograph.

The gamma detector was always mounted level and aimed directly at the column axis with its collimating orifice 7 ft-2 in. from the column axis. After positioning and shortly before shot time, the system performance was checked with a low-level Cs^{137} standard source placed in the lead collimator orifice. In addition, the triggering levels of the oscilloscopes being used as energy discriminators were set by bringing Au^{198} tracer within range of the detector to provide sufficient photons of characteristic energy. The system was tested for spurious pulses which might result from firing of the samplers and from explosive shock effects, by operating the system during a shot without tracer.

C O N F I D E N T I A L

Sample Treatment

After each shot the sampler reservoirs were opened and the samples removed in the following manner. When a reservoir contained a large volume of liquid, its volume was measured with a graduate. All of the sample was stored in a polyethylene bottle from which a smaller sample was drawn later for counting. Samples with volumes of 10 to 100 ml were also measured with a graduate and then stored in a 100-ml lusteroid tube that could be inserted directly into the well-counter. Samples of 10 ml or less were measured with a small graduate and then poured into a lusteroid tube. In order to assure recovery of all tracer for these small samples, the sampler reservoir and cap were rinsed with distilled water and swabbed with a paper tissue, all of which also was placed in the lusteroid tube for counting.

All samples then were counted immediately in a standard 3-in. well crystal counter system to determine the gross count rate of the sample. This gross count rate was then corrected for counter background, sample volume, decay of tracer, and pre-shot pond water background to yield a total count rate for the sample.

Correction for pond background required samples prior to each shot. When two shots were fired the same day, the background samples for the second shot were taken just prior to the second shot. To ensure sufficient mixing, both pond filter systems were used to circulate the pond water after each shot.

C O N F I D E N T I A L

RESULTS

TRACER DISTRIBUTION

The tracer sampling data for each shot consisted of 15 samples: two samples at each of 7 sampling radii (right and left) and the center axis sample. It was desired to reduce the data so as to obtain a radial distribution and a time history of the tracer arrival for each charge depth and sampling level. Because of the many combinations of charge depth, sampling height, and termination time, it was possible to fire only a few shots for each particular combination due to limitations of time and funds.

The few samples (1 to 8) at each combination (charge depth, sample position and termination time) generally presented a large range of values so that it was difficult to determine the time increment during which tracer actually arrived. This resulted from the cumulative mode of sampling employed. With so few samples at each condition, no conventional statistical methods could be applied; so a sample averaging process was employed in the following manner. First, all samples were normalized to sample counts per minute per millicurie of tracer inserted into the charge. Then all the sample values for like shot combinations of depth, sample position and termination times were arithmetically averaged together (samples taken with the 3/8 in. orifice were corrected to the standard sampler area). Next the average value for the shortest sampling termination time (at a given sample position and charge depth)

C O N F I D E N T I A L

C O N F I D E N T I A L

was compared with the average value of the next longer time to see whether a significant increase was evident. Generally, a 20 % increase in the average value was considered significant; but in the cases where the average value for the longer period showed a lesser increase, values for both times were averaged together and assigned to the earlier time period. This assumes that no significant additional tracer was collected during the longer time period. The averaging process was continued for successively longer sampling times until a 20 % increase occurred, and a new average value was established. This process had the advantage of utilizing all possible data.

The results of this data analysis are presented in Figs. 3.1 to 3.3 for the three shallowest charge depths, 1.6, 2.5, and 3.5 in. Each figure shows two distributions, A and B, one at each of the two established sampling heights (h_s). The tracer distributions for deeper charge depths, 5.5 in. and greater, are not presented because the maximum quantity of tracer was only a few percent of that measured at the shallower depths.

TOTAL TRACER IN COLUMN

With the radial distribution of tracer now established, the total fraction of tracer transferred to the column can be computed for each specific sampling height and time. This computation, which assumes symmetry about the vertical axis, divides the horizontal cross-section of the column into a 3-in. radius circle and seven 6-in. wide concentric rings, each ring having a mean radius corresponding to successive sampling stations. The sample count rate at each sampling radius, which is proportional to the quantity of tracer, is multiplied by the area factor of the ring. Then the products for all rings are summed to give the total count rate per millicurie of input tracer. The counter efficiency for the tracer (53 %) being known, the total count rate is converted to

C O N F I D E N T I A L

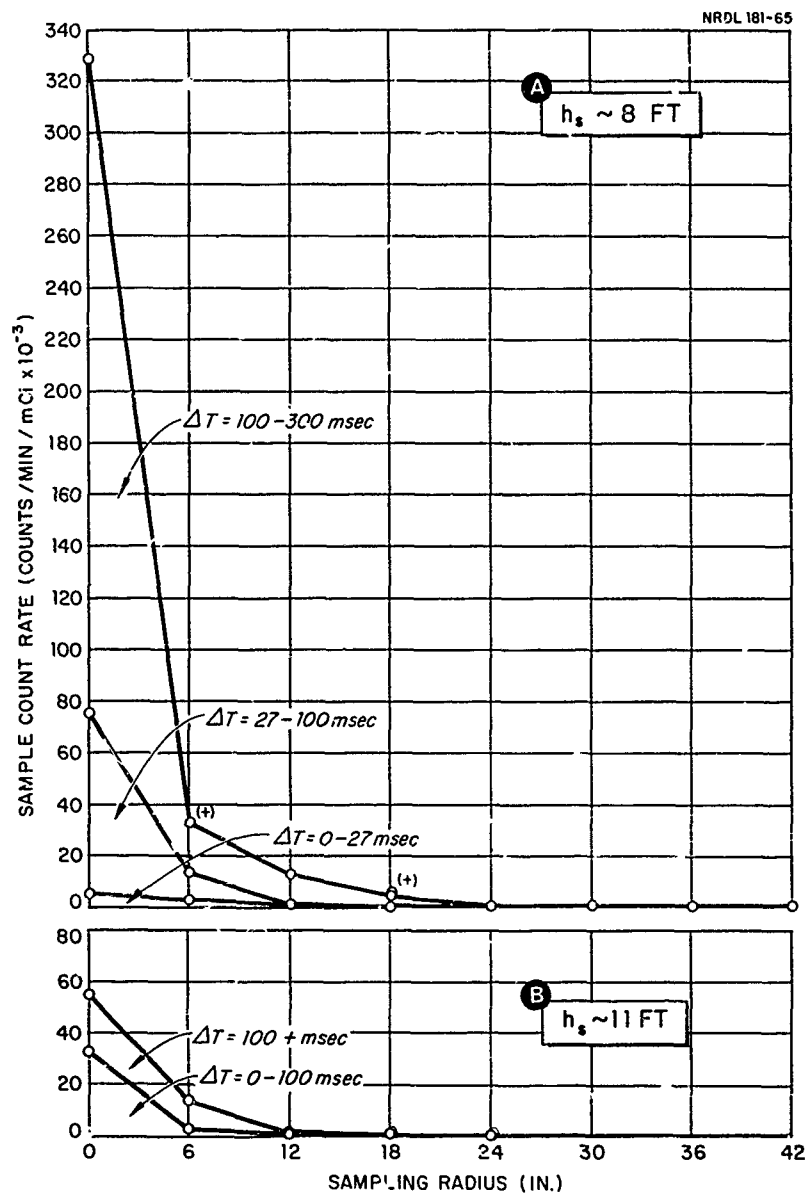


Fig. 3.1 A & B Sample Count Rate Per Millicurie of Tracer vs. Column Radius for 1.6 in. Charge Depth

C O N F I D E N T I A L

C O N F I D E N T I A L

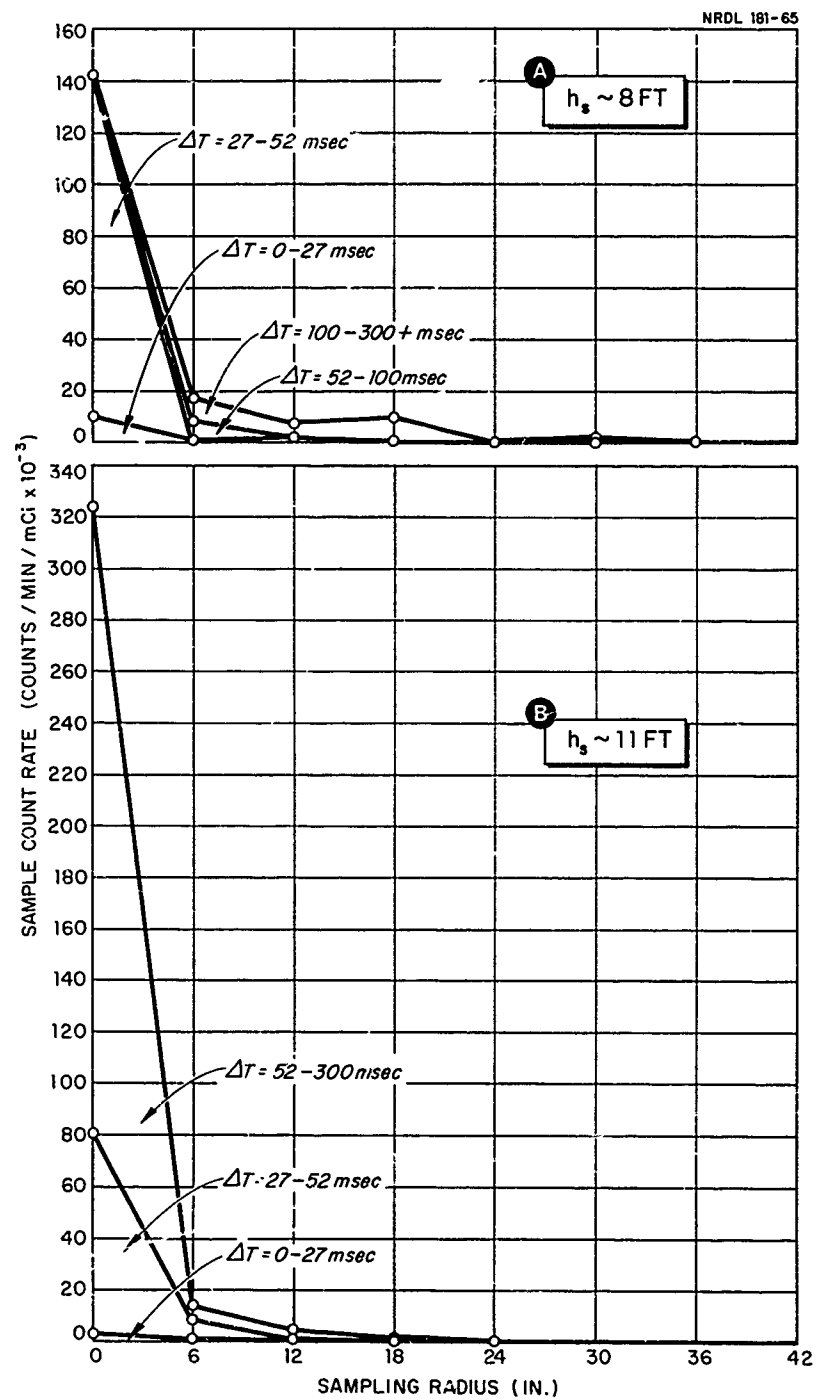


Fig. 3.2 A&B Sample Count Rate Per Millicurie of Tracer vs. Column Radius for 2.5-in. Charge Depth

C O N F I D E N T I A L

C O N F I D E N T I A L

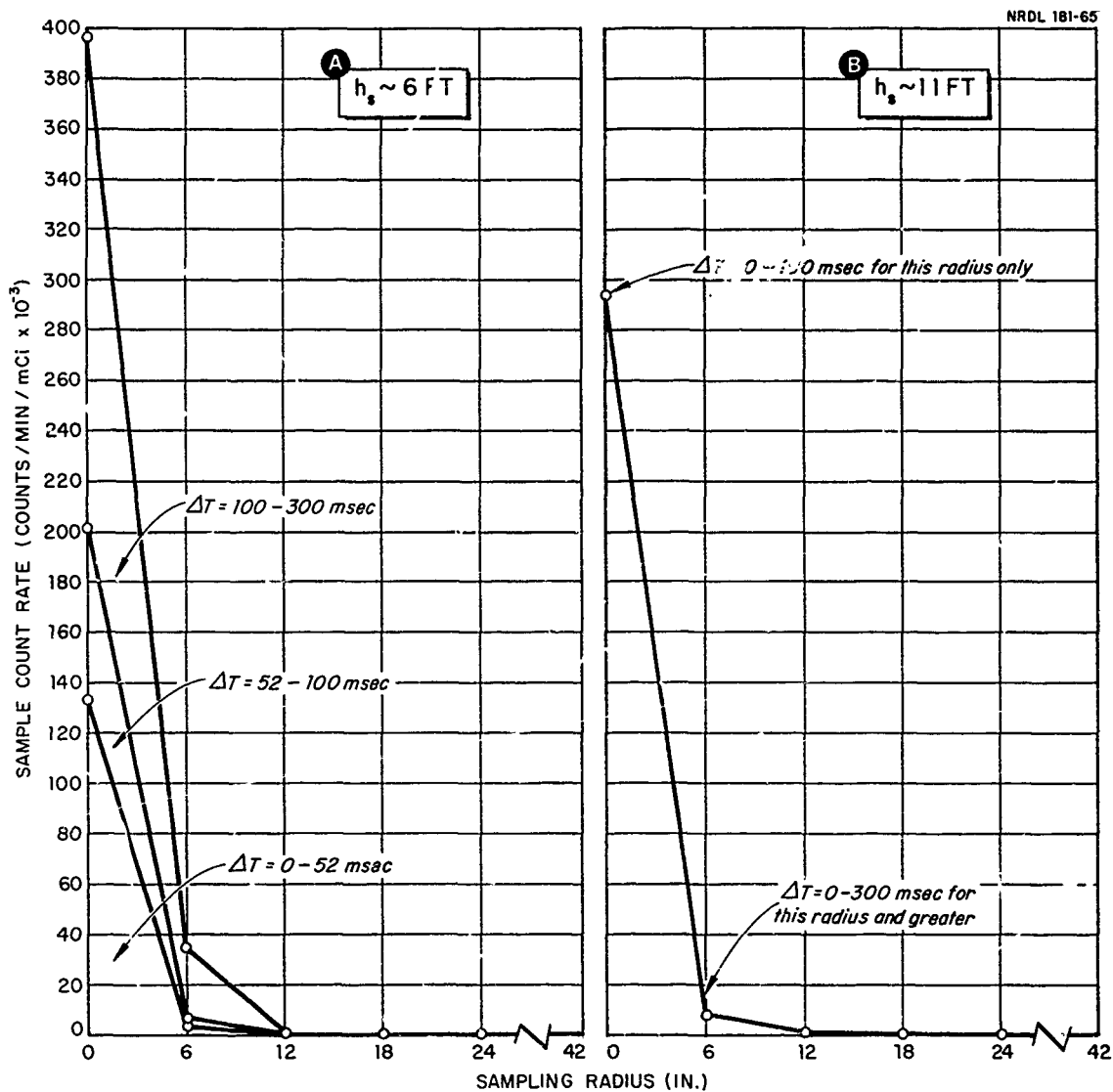


Fig. 3.3 A&B Sample Count Rate Per Millicurie of Tracer vs. Column Radius for 3.5 in. Charge Depth

C O N F I D E N T I A L

C O N F I D E N T I A L

disintegrations per minute, and then divided by the defined number of disintegrations per millicurie to get the fraction of tracer resulting at this specific condition. These results are presented in Table 3.1 for all combinations of conditions for which sufficient data was available.

The total fraction of tracer in the column from Table 3.1 has been plotted, Fig. 3.4, against charge depth at the lower nominal sampling heights of either 5 ft-8 in. or 7 ft-8 in. depending on charge depth for all available times, so as to present more clearly the time development of the tracer transfer process. It should be noted that the fraction of tracer presented is cumulative with time. Therefore, the maximum quantity of tracer would be only approximately 5 %.

The data from Table 3.1 is also plotted, in Fig. 3.5, against time for a charge depth of 2.5 in. at both nominal sampling heights of 8 and 11 ft to show the similarity of the time history at each sampling height. Since no data is available between 100 and 300 msec, that section of the curve was interpolated and is shown in dashed lines.

A crude estimate of the tracer remaining in the pond after a shot was made by taking several samples of pond water after the tracer had an opportunity to mix with the water for an hour or more. After counting the samples and adjusting for preshot background and counter efficiency, the total fraction of tracer remaining could then be calculated, the total volume of water in the pond being known. The resulting estimated fraction of post-shot tracer in the pond has been plotted against charge depth in Fig. 3.6 for all shots where data was available. The scatter of data seems to be rather wide for all the charge depths. A crude curve was drawn through the average of all points, and it is seen that the smallest post-shot fraction of tracer occurs at the shallowest charge depths while there is no apparent loss at a depth of 5.5 in. It should

C O N F I D E N T I A L

C O N F I D E N T I A L

TABLE 3.1
Fraction of Tracer in Column (%)

Charge Depth (in.)	Sampling Height	Sample Termination Time (msec)				
		27	52	100	300	Total Event
1.6	7'-8"	0.4	-	1.2	5.4	-
1.6	10'-8"	-	-	0.4	-	1.0
2.5	7'-8"	0.5	1.2	1.5	3.9	-
2.5	10'-8"	0.2	1.0	1.3	3.3	-
3.5	5'-8"	-	0.9	1.6	3.8	-
3.5	10'-8"	-	-	2.0	-	-
5.5	5'-8"	-	0.02	-	0.1	-
7.5	5'-8"	-	-	0.02	-	-

C O N F I D E N T I A L

C O N F I D E N T I A L

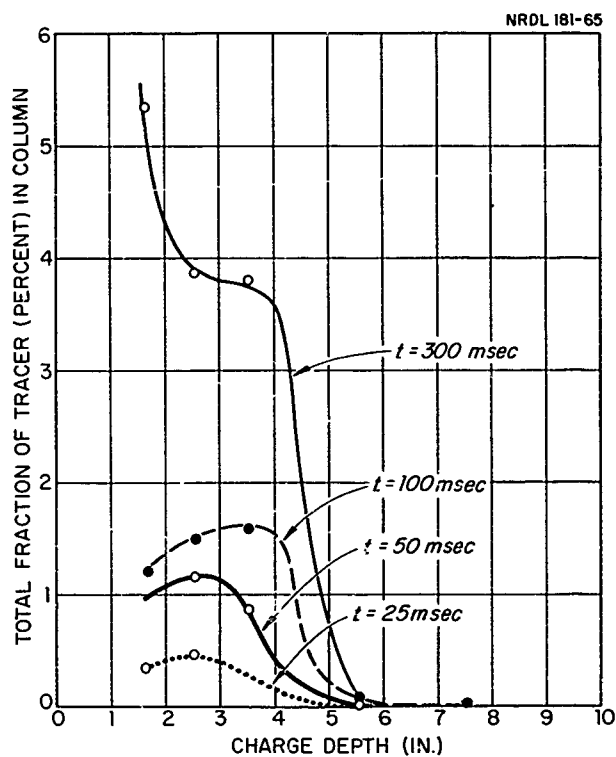


Fig. 3.4 Total Fraction of Tracer in Column vs. Charge Depth for Nominal Sampling Height of 6 or 8 ft

C O N F I D E N T I A L

C O N F I D E N T I A L

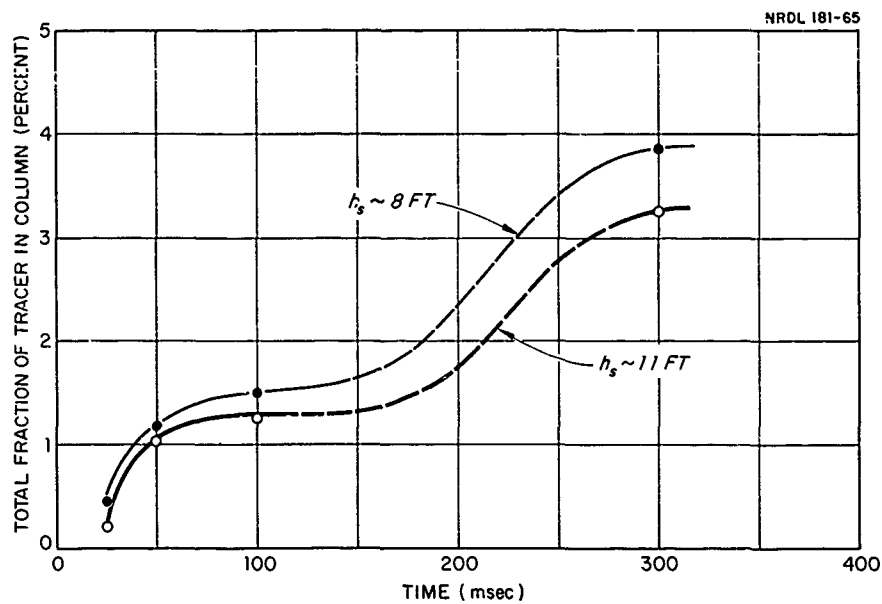


Fig. 3.5 Total Fraction of Tracer in the Column vs. Time for 2.5-in. Charge Depth

C O N F I D E N T I A L

C O N F I D E N T I A L

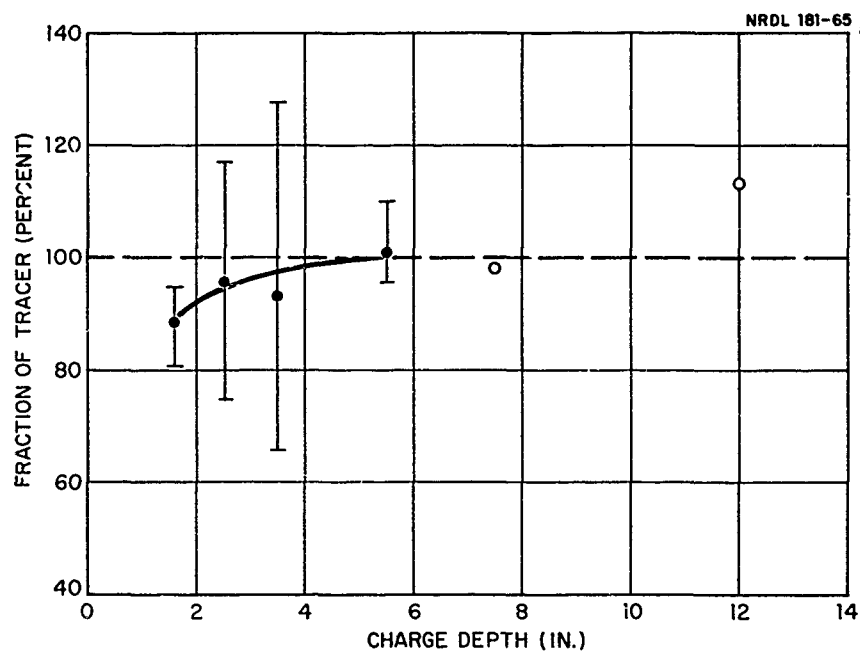


Fig. 3.6 Post-Shot Fraction of Tracer in the Pond vs. Charge Depth

C O N F I D E N T I A L

C O N F I D E N T I A L

be pointed out that the post-shot fraction of tracer would not include any tracer in water which fell beyond the pond surface and therefore would depend on wind conditions.

WATER DISTRIBUTION IN THE COLUMN

Water volume data is of course a by-product of the tracer sampling data that was of primary concern during this experimental phase; however, it is useful as supplementary data for determination of the internal column structure. The column structure had been determined by water sampling previously but the data was sparse, particularly at the shallow charge depths of 1.6 and 2.5 in. where most of the tracer work was accomplished. In view of this, it is considered worthwhile to use the additional water volume data to revise or extend the radial distributions of water in the columns presented in Ref. 1. The new sample volume data was combined with the previous data for each condition of charge depth and sampling height and then reduced in the same manner as the tracer data, so as to distribute the cumulative sample volume into appropriate time intervals. The resulting radial distributions of sample volume per standard 3/4-in. snout orifice are presented in Appendix A for charge depths of 1.6 to 12 in. and sampling heights where new data was available.

The revised and extended water volume distributions within the column provided the opportunity to up-date the values of total ejected water in the column which also had been presented in Ref. 1. The total ejected volumes were calculated as before by numerical integration of the radial volume distributions for each condition of charge depth, sampling height, and time within event. A table of cumulative total ejected water is presented in Appendix A, which includes values for all conditions

C O N F I D E N T I A L

where sampling data is available. The table is coded as noted to show new, revised, and unchanged values from Ref. 1. The new and revised data does not indicate any significant changes in the results of Ref. 1.

GAMMA RADIATION ADJACENT TO THE COLUMN

Radiation measurements, made with the collimated gamma detector mounted adjacent to the rising column, were made as an additional means of locating the tracer within the column. Since the radiation levels were quite low and the total event time was short (1 to 2 sec), considerable care was taken when reducing the pulse data to count rates because of the critical effect of the time interval over which pulses were counted. As previously discussed, pulses from the scintillation gamma detector were recorded directly on the oscillograph record. So, except for inefficiencies, each pulse recorded represents a gamma photon striking the detector.

The radiation record for each shot was first reduced by counting all pulses in each 100-msec interval starting at zero time and then normalizing to a 20 millicurie tracer input. The number of pulses per time interval for all similar conditions of charge depth and detector height, or a small range of heights in some cases, were then averaged together and plotted against time. The resulting graphs for each charge depth have been made with the data for the different detector heights superimposed and the pulses per 100-msec interval converted to counts/sec. No correction has been made for counting system efficiency, and data is not given for detector heights above 66 in. because in this region the count rates were not significantly above background. The results do not change noticeably with charge depth; so only those for the 1.6 in. charge depth are given in Fig. 3.7, while the remainder are given in Appendix B.

C O N F I D E N T I A L

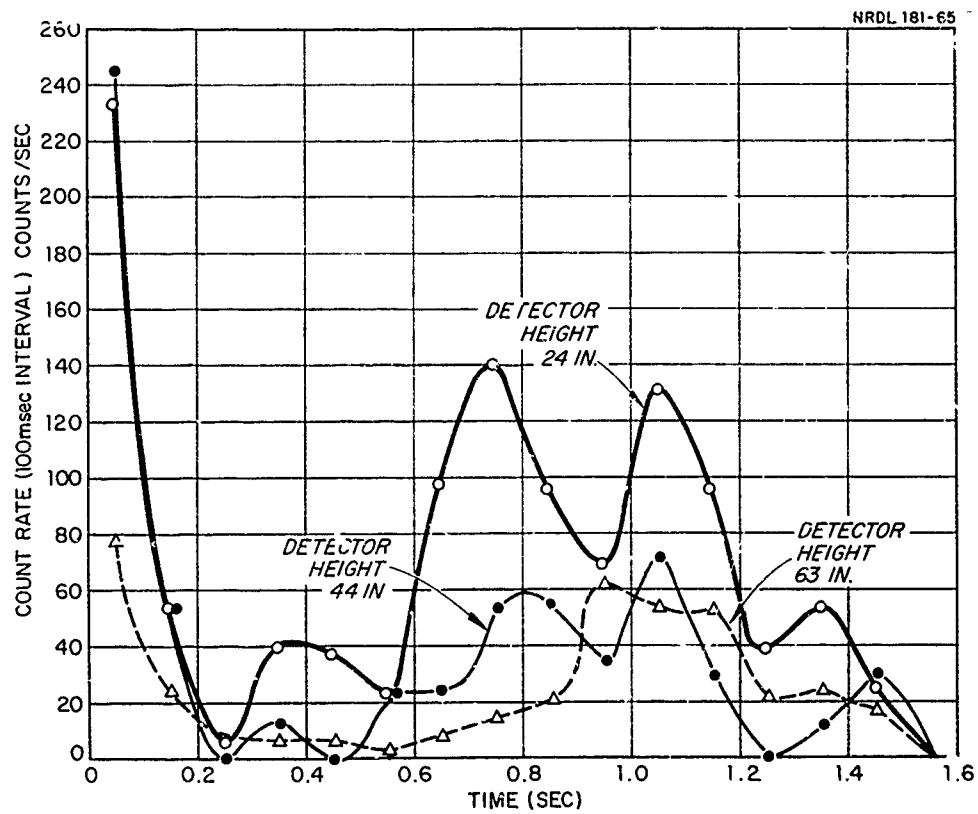


Fig. 3.7 Gamma Count Rate (per 100-msec interval) vs. Time for 1.6-in. Charge Depth

C O N F I D E N T I A L

C O N F I D E N T I A L

Close examination of the number of counts during the first 100 msec interval shows a sharp reduction with increasing detector height. This effect is shown in Fig. 3.8, where the number of counts (or pulses from the record) for the first 20 msec of the event, normalized to the standard 20 millicurie input, is plotted vs. detector height above the water surface for all shots at the 2.5 in. charge depth. The sharp cut-off between 5 and 6 ft indicates the initial maximum height reached by the tracer within the column. Similar graphs for charge depth of 1.6 and 3.5 in. are given in Appendix C.

The initial high count rates during the first 100 to 200 msec at detector levels below 6 ft were analyzed more intensively so as to gain both high time resolution and a true indication of count rate. This was accomplished by measuring the "time between pulses" directly from the records, and then plotting its inverse, which is count rate (counts/sec) vs. time both on a log-scale. The count rate point was plotted at the mid-time between the pulses from which it was derived. All data available for each condition of depth and detector height was plotted on a separate graph, and then a best curve was drawn in through the points. The resulting curves (minus the data points) were then combined for each charge depth into one graph which included the curves for all detector heights. This arrangement allows convenient examination of the relative time of peak count rates for each detector height. Figure 3.9 is a typical high resolution initial count rate graph for a charge depth of 2.5 in., with curves for detector heights of 18 and 44 in. and approximately 5 ft. The three separate plots for each detector height at the 2.5-in. charge depth which show all the data points and resulting curves are given in Appendix D. The remaining plots of combined high resolution initial count rates for charge depths of 1.6, 5.5 and 7.5 in. are also presented in Appendix D.

C O N F I D E N T I A L

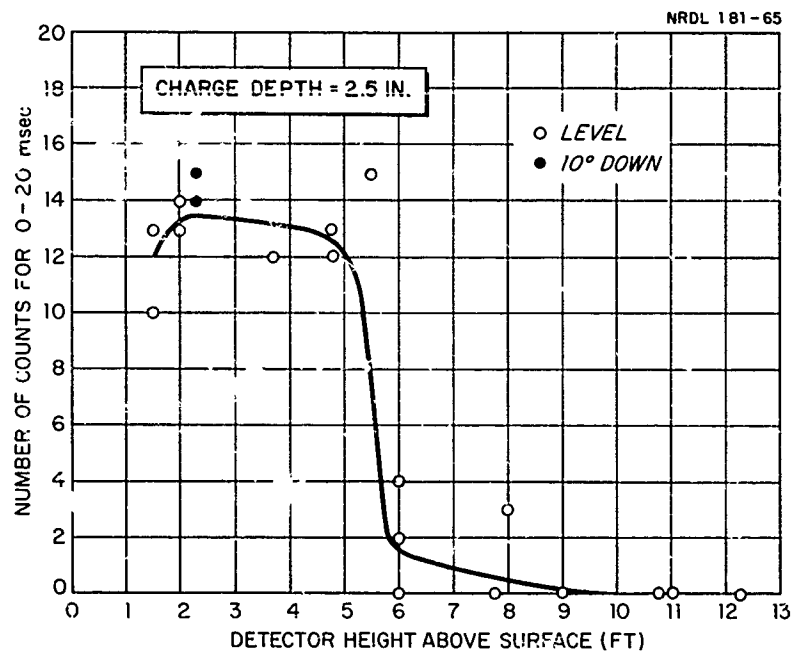


Fig. 3.8 Number of Counts During the First 20 msec vs. Detector Height Above Surface for 2.5-in. Charge Depth

C O N F I D E N T I A L

C O N F I D E N T I A L

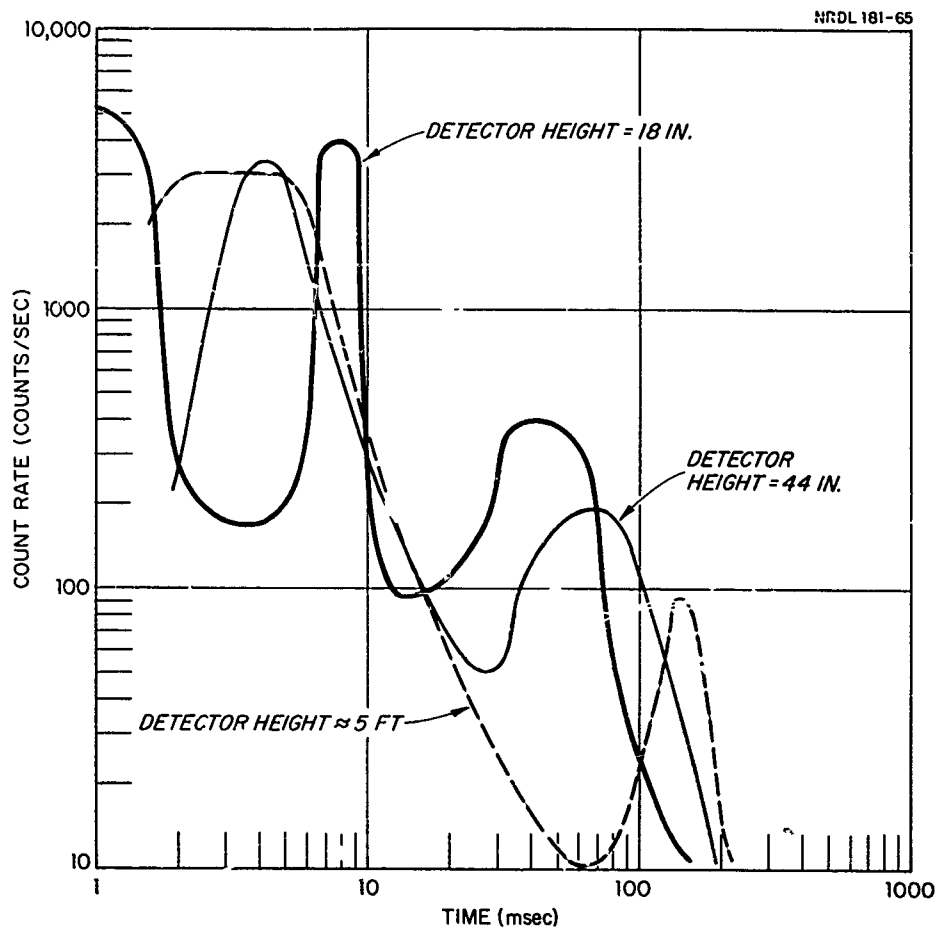


Fig. 3.9 High Time-Resolution Count Rate vs. Time for Initial 200-msec Period at 2.5-in. Charge Depth

C O N F I D E N T I A L

C O N F I D E N T I A L

ANALYSIS AND DISCUSSION

TRANSFER AND DISTRIBUTION OF TRACER BY SAMPLING

The radial distributions of tracer at two sampling heights have been presented in Figs. 3.1 to 3.3 for charge depths of 1.6, 2.5 and 3.5 in. Distributions were not presented for charge depths of 5.5 in. or deeper, because no significant quantity of tracer was present in the samples. These radial tracer distributions typically have a low initial level all across the column during the first time interval (0 to 27 msec), followed by a rapid increase during subsequent time intervals at the column center.

The only exception to this rather typical tracer distribution occurs in Fig. 3.2A, where no increase in tracer is evident at the column center after 52 msec, where typically a large increase out to 300 msec would be expected. A review of the data incorporated in Fig. 3.2A shows that in an attempt to resolve the problem, 3 shots were fired with sampling terminated at 300 msec. The highest sample count rate at zero radius was 216×10^3 counts/min/mc, which is seen to be less than the typical peak values of 300×10^3 or more. It was not possible to fire additional shots at this condition to clear up this troublesome piece of data; so it will be assumed that the radial tracer distribution is similar to the others and that additional data would show this to be the case.

C O N F I D E N T I A L

C O N F I D E N T I A L

This typical radial tracer distribution - very low amounts all across the column at early times followed by very large quantities at the column center during the 50 to 300-msec period - is seen to be strikingly similar to the water distributions. This similarity is readily observed by simple comparison of the tracer distributions in Figs. 3.1 to 3.3 with the water sample volume distributions either in Appendix A or those from the earlier sampling experiments given in Ref. 1. It must be added that the similarity of the distributions holds only to depths of 3.5 in., because no significant amount of tracer is transferred into the column at depths of 5.5 in. and deeper.

This previous sampling work had clearly established that for one-pound charges at shallow depths the upward flowing column walls converged at a height of approximately 6 ft into a high velocity, central jet. All of the tracer sampling was done at the convergence height or higher so that the large water volumes and tracer samples collected at the column center are from the central jet. It must be concluded then that since the water in the central jet comes from the lower column walls, the large quantity of tracer found in the central jet must also have been associated with the column walls.

The total fraction of the input tracer transferred into the column and crown as computed from the tracer distributions has been presented in Fig. 3.4 for the standard charge depths and event times. It is apparent from this figure that the total fraction of tracer transferred into the column is 5 % or less, with all but 1/2 % or less collected after 27 msec. This would indicate that the largest fraction of the total tracer found in the column and crown is transferred via the upward flowing column walls.

Figure 3.6, which gives the post-shot fraction of tracer found in the pond, should be considered along with the data for the total fraction

C O N F I D E N T I A L

of tracer transferred into the column, since the unaccounted-for fraction may represent an additional quantity of tracer present in the column but which escaped sampling. For the shallowest charge depth (1.6 in.) the missing fraction of tracer is 10 to 12 %, which must be seriously considered because it exceeds by a factor of 2 the total quantity of tracer in the column as measured by sampling. There are several opportunities for tracer to be lost during the event and not be returned to the pond water: (a) direct venting of the tracer in gaseous form or as a very light aerosol during the initial column formation; (b) inclusion of tracer in the light crown aerosol, much of which is blown downwind; (c) fallout of tracer included in the central jet or column walls outside the pond; (d) venting in a gaseous or light aerosol form during the final bubble venting or late emission processes; (e) loss to the pond surfaces or filter system.

Some pertinent considerations concerning loss of the tracer from the pond can be discussed at this point. First, loss to pond surfaces or filter system need not be considered, because tests with the Au¹⁹⁸ tracer showed no uptake over a period of several days. Next, the loss due to fallout of the main column outside of the pond cannot be of great significance because the bulk of the column water which contained, at most, 5 % of the tracer did return to the pond.

Another possibility is that the lost fraction of the tracer was included in the crown aerosol, most of which was blown downwind. This condition would require that the sampling measurements made at the crown height (~ 11 ft) be very inefficient, thus resulting in a low value of total tracer in the column. The possibility of inefficient sampling in the crown is very real considering the unknown flow patterns within the crown; however, sampling below the crown height, where the flow is known, gives very similar results. This is shown nicely in Fig. 3.5 where the total fraction of tracer is given with time for both

C O N F I D E N T I A L

8- and 11-ft sampling levels, and the variation is only 13 % at 100 msec. Further consideration will be given to the fraction of tracer lost from the pond later in the report.

GAMMA RADIATION ADJACENT TO THE COLUMN

Measurements with the collimated gamma detector adjacent to the column at various levels were made as a supplemental means of determining the distribution history of the tracer in the column. Typical gamma records are shown in Fig. 3.7 for several detector levels at the 1.6-in. charge depth. These records for the complete event show a characteristic initial pulse of radiation during the first 100-msec interval, followed by a drop to background level until 500 to 600 msec and then a moderate increase until about 1.5 sec. The peak radiation count rates diminish with successive increases of detector height or equivalent column height until approximately a height of 6 ft, where the count rates approach background levels. Measurements were made at heights up to 12 ft, which is about the center of the fully developed crown for a very shallow charge depth.

The initial radiation pulse will be considered in detail first, since it is associated with the column formation processes. The secondary radiation peak which occurs during the final stages of the event will be considered later. The first analysis of the initial pulse was aimed at determining more precisely its characteristic decrease with detector height. This was done in Fig. 3.8, where the total number of counts during the first 20 msec of the event is plotted for all detector heights at the same charge depth, and the result is a rather sharply defined cut-off between 5 and 6 ft. A very similar cut-off of radiation at about the same height is seen from the 1.6- and 3.5-in. charge

C O N F I D E N T I A L

depth data given in Appendix C. At this point it must be concluded that the bulk of the tracer does not move above this cut-off height within the column.

Consider next the plots of high resolution count rate vs. time for the period of the initial pulse (20 msec) presented in Fig. 3.9. Examination will reveal the following pertinent facts: (a) the curve for the lowest detector height (18 in.) peaks first at 1 msec and then again at about 8 msec; (b) the next higher detector curve (44 in.) shows only a single peak at an intermediate time of 4 msec; (c) the highest detector curve (5 ft) has a broad intermediate peak; (d) the peak count rates in all cases are between 3,000 and 5,000 counts/sec. These relative-time locations of the count rate peaks for different detector heights, considered along with the sharp cut-off of radiation at 5 to 6 ft, can be interpreted only as a rapid upward movement of the tracer within the column to the cut-off height, followed by a reversal downward mostly back below the water surface. Most significant in this interpretation is the double peak of the lower detector curve, indicating the first passage of the tracer during its upward movement and then its return downward.

As for the fraction of the total tracer involved in this initial motion and its radial distribution, the collimated detector response for several geometrical distributions of the tracer within the column was calculated, assuming a nominal 20 millicuries of tracer, axial symmetry, and no water shielding to see what distribution best fit the data. These calculations clearly established that the maximum count rate response of the detector in its normal position with respect to the column occurs when the tracer is located at the vertical column axis within a spherical volume of diameter not larger than 6 in. At this geometry, which is for all practical purposes a point source, the calculated count rate is a maximum of 6,700 counts/sec. This maximum count rate exceeds

C O N F I D E N T I A L

C O N F I D E N T I A L

the observed peak rates of 3,000 to 5,000 counts/sec for the various detector heights during the upward excursion of the tracer by only a small factor. Therefore it must be concluded that: (a) all the tracer is involved in the upward excursion; (b) the tracer is in a small core which moves along the vertical column axis; and (c) during the excursion and downward reversal the tracer core may smear along the vertical axis. Thus, the tracer in a relatively small core is seen to make an above-water excursion within the column to a height of approximately 5 ft at 3 to 4 msec and to return below-surface by 10 to 15 msec.

In order to see the tracer excursion with respect to the early column and bubble development, the tracer position as deduced from plots of count rate vs. time (Fig. 3.9 and Appendix D) has been superimposed on typical bubble and column outlines for similar firing conditions at charge depths of 1.6, 2.5 and 5.5 in. These outlines are taken from high speed above- and below-surface films. The results for the respective depths are presented in Fig. 4.1 where an outline and tracer position are given at event times of 1, 2, 3, 5 and 10 msec - except for the 5.5-in. depth where the sequence starts at 2 msec. The tracer core is seen to make an upward excursion into the column at all three depths and remains inside the column boundary except for the shallowest charge depth of 1.6 in. At this depth the column at 1 msec appears to be open-topped, with the luminescent explosion products visible and the tracer core located very near the upper column boundary among the exposed explosion products. The following outline at 2 msec shows that the top of the column has moved upward ahead of the tracer core.

Further inspection of the initial tracer excursions shown in Fig. 4.1 will show that the tracer core reaches its maximum height more quickly at the shallower charge depths. To examine this effect more fully, the tracer reversal time or the time of maximum height was determined for all charge depths for which data was available. The reversal

C O N F I D E N T I A L

time was determined from inspection of the curve for the lowest detector height on plots of the high resolution count rate vs. time (Fig. 3.9 and Appendix D) and was taken to be time of minimum count rate between the typical twin peaks. This approach was taken in lieu of determining the time of maximum count rate for the highest detector height because the minimum was more sharply defined in most cases. These reversal times were then plotted in Fig. 4.2 along with the predicted bubble top half-period from the non-spherical bubble model (Ref. 2) for charge depths to 1 ft. There is no tracer reversal time shown at the 12-in. charge depth, because the available measurements were limited to detector heights of 44 in. where no initial radiation pulse was observed.

The tracer reversal times for charge depths between 1.6 and 7.5 in. show very good agreement with the predicted bubble top half-period, and therefore, it can only be concluded that the tracer excursion - and thus the initial radiation pulse - is associated with the motion of the upper bubble boundary. Further, the top bubble period as calculated from the bubble model accurately describes the time and duration of the initial radiation pulse.

TRANSFER MECHANISMS OF EXPLOSION PRODUCT
TRACER INTO THE COLUMN

In this section three distinct modes or phases of tracer transfer will be suggested, and then each will be discussed. The supporting discussion of each transfer mode will make use of the experimental data presented in this report along with concepts of internal column structure, mostly from Ref. 1. In some cases where gaps in the data exist, the author's experience has been utilized in order to present a completed concept. Also, several other sources have been used and are appropriately referenced. The objective here is to go beyond merely reporting

C O N F I D E N T I A L

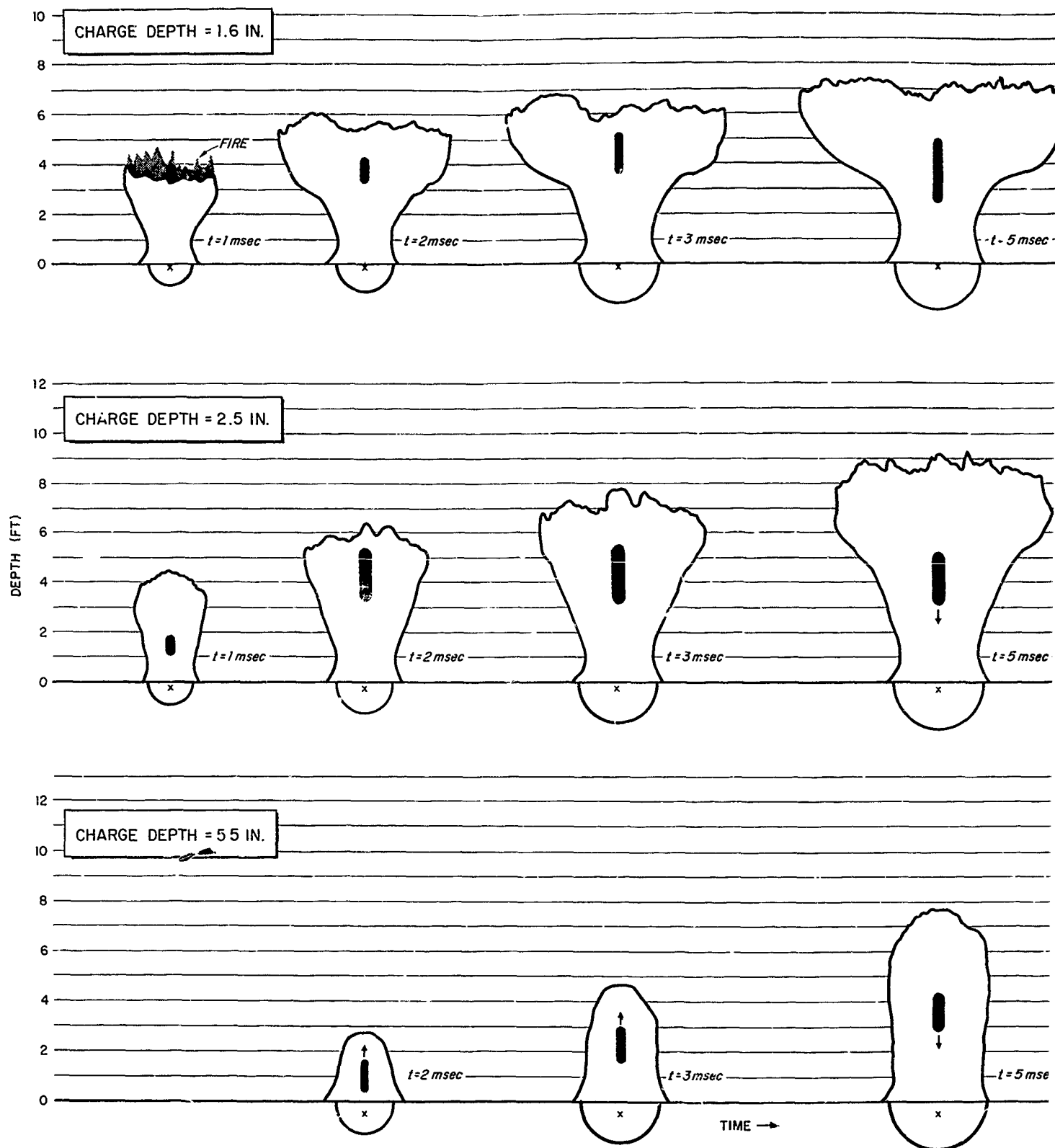


Fig. 4.1 Tracer Location Within Column During the Initial Excursion Period, for Charge Depths 1.6, 2.5 and 5.5 in.

C O N F I D

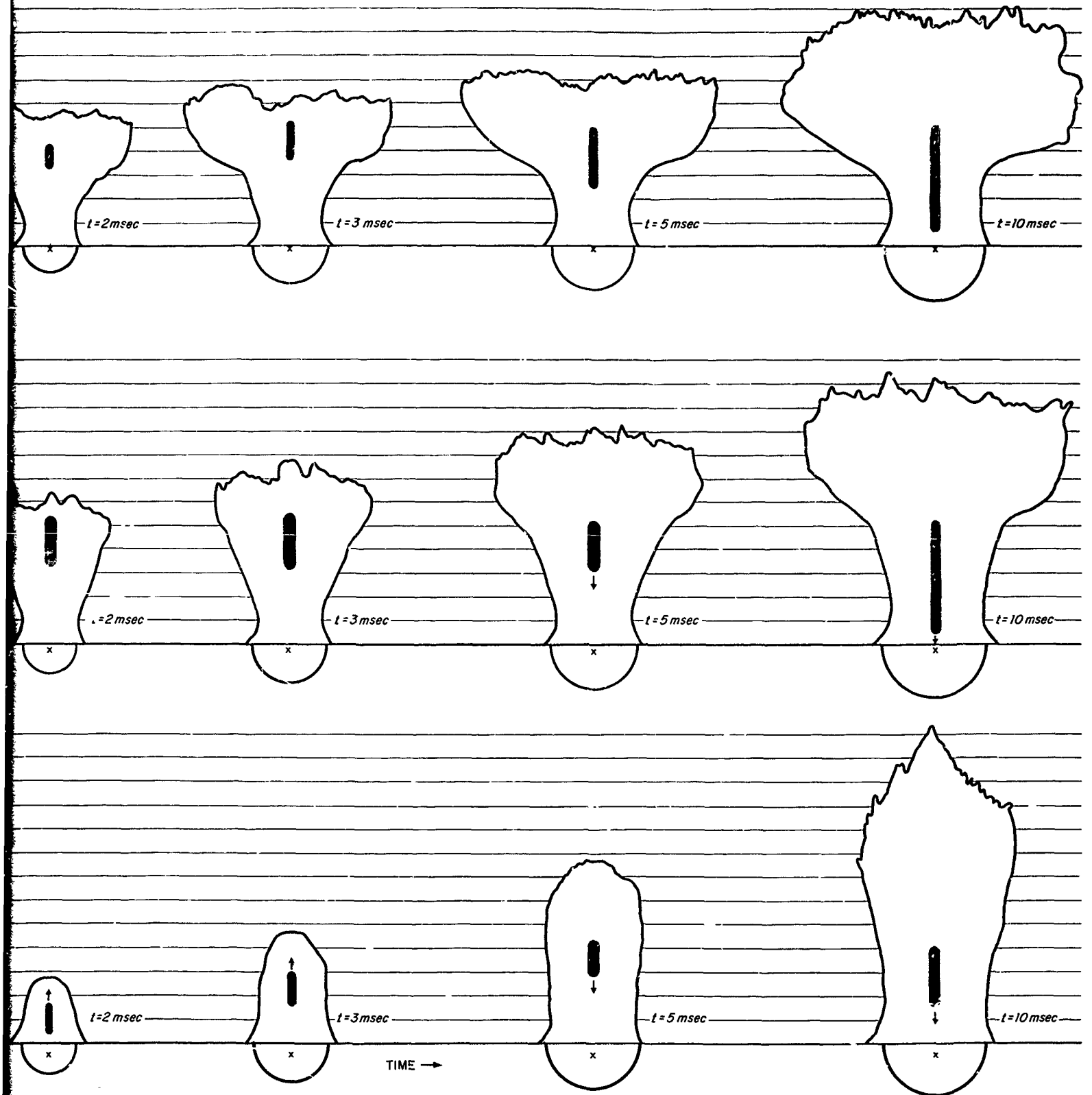


Fig. 4.1 Tracer Location Within Column During the Initial Excursion Period, for Charge Depths 1.6, 2.5 and 5.5 in.

CONFIDENTIAL

2

45.46

C O N F I D E N T I A L

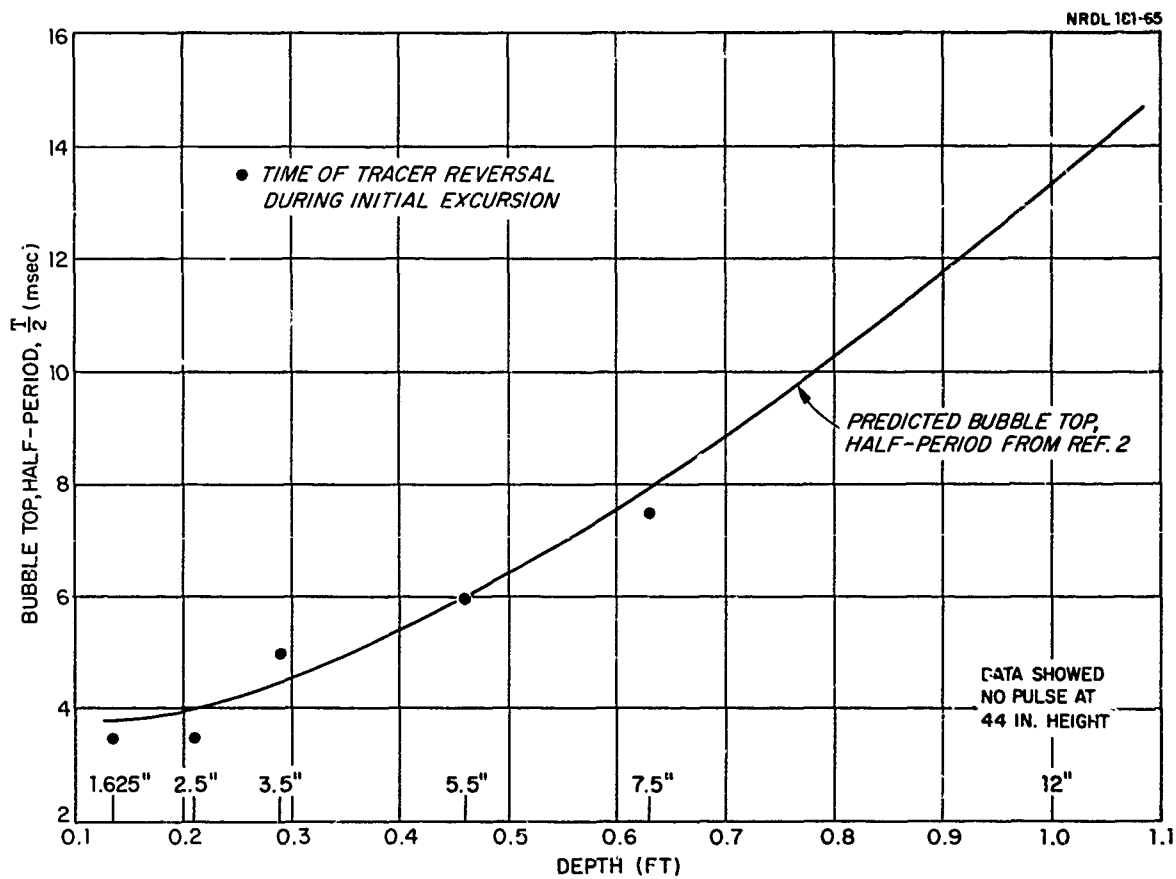


Fig. 4.2 Predicted Bubble Top Half-Period vs. Charge Depth with Tracer Reversal Times at Standard Charge Depths

C O N F I D E N T I A L

C O N F I D E N T I A L

experimental data and advance some concepts on the mechanisms by which explosion products are transferred into the column and crown. This report does not include any quantitative data on the third transfer phase; however, it has been included so as to make the discussion as comprehensive as possible.

First, the three transfer phases will be defined, and then a sequential series of schematic drawings will be presented with discussion to illustrate the transfer mechanisms.

Phase I - Transfer into the crown or upper column during the period of the initial upward excursion of the tracer core within the column.

Phase II - Transfer into the upward flowing column walls from the below-surface bubble after return of the tracer to the bubble from its initial upward excursion.

Phase III - Transfer to the late emission plumes as the underwater bubble collapses upward from the bottom.

For shallow one-pound explosions, these transfer phases are separated in time so that it is possible to construct a series of schematic drawings to show how the transfer processes are associated with the column-bubble hydrodynamics. Such a series of illustrations is presented in Fig. 4.3 for a charge depth of 2.5 in., which roughly scales Cross-roads-Baker geometry in a bottom-free environment. The time sequence of drawings was constructed using photographic data⁶ for outlines of the bubble and column, tracer sampling data, radiation detector data, and the general hydrodynamic features of the column and bubble as previously established. Referring now to Fig. 4.3, each event time shown will be discussed:

1 msec. The column is now in a stage of early development. The explosion products and the tracer core are contained within the upward flowing column walls, while the tracer core is seen to be at about half

C O N F I D E N T I A L

C O N F I D E N T I A L

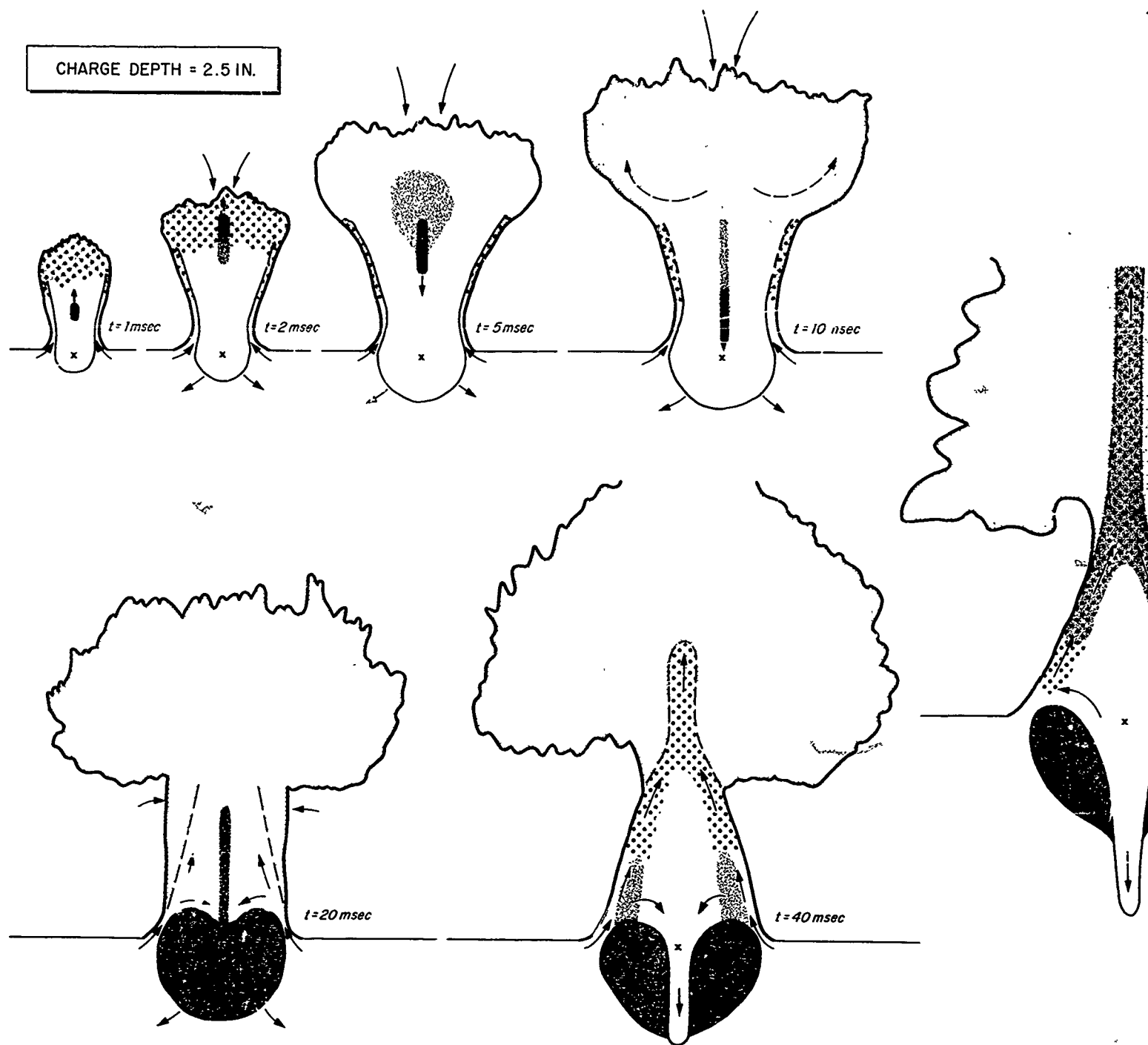
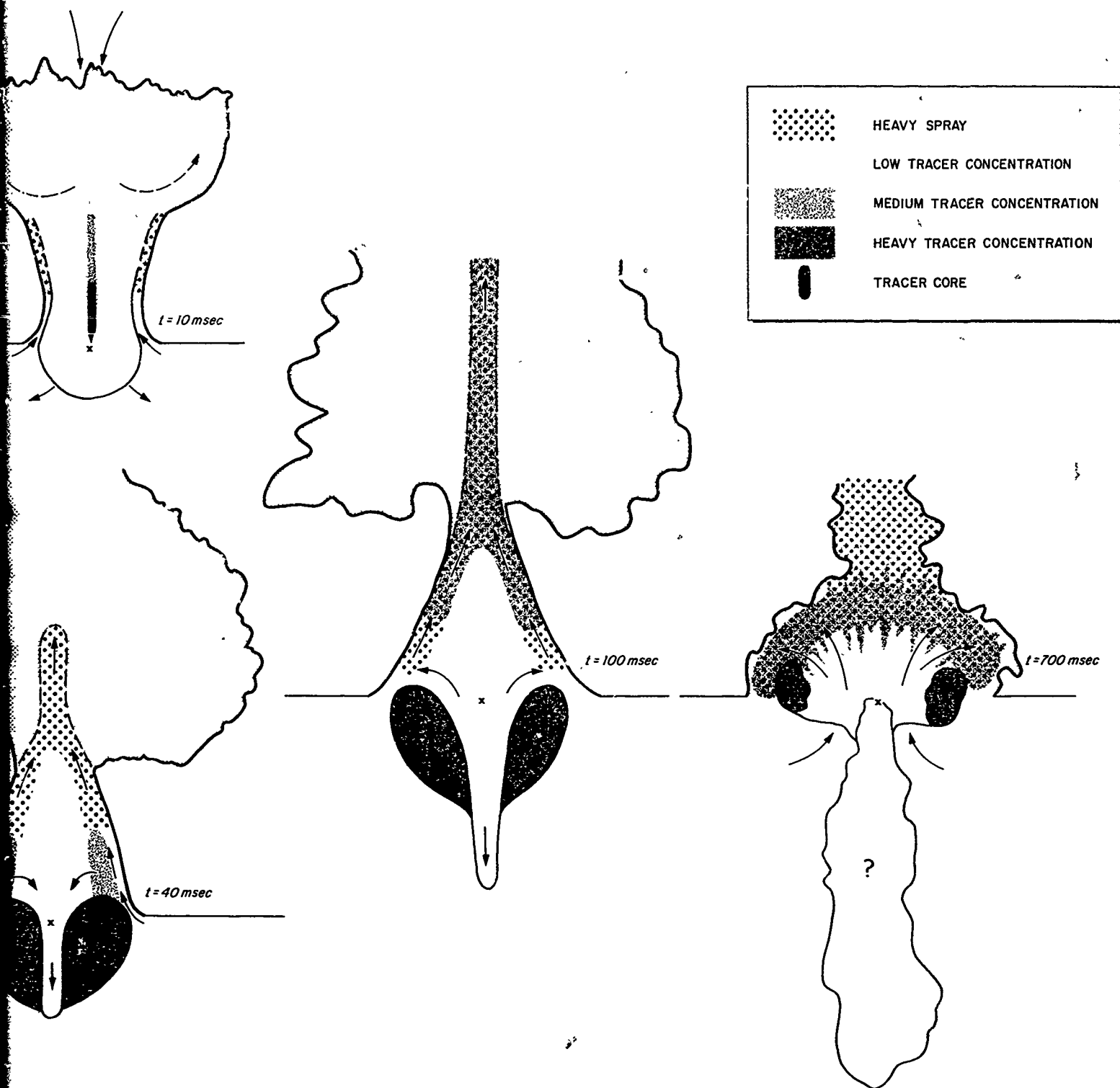


Fig. 4.3 Schematic Illustrations of Explosion Product Transfer Hydrodynamic Processes for Charge Depth 2.5 in.



Schematic Illustrations of Explosion Product Transfer and Related Processes for Charge Depth 2.5 in.

49-50

C O N F I D E N T I A L

C O N F I D E N T I A L

the column height and moving upward. The column is topped with a heavy water aerosol which consists of the initial layer of water over the charge. Escape of explosion products from the column top would not be expected at this time because the internal gas pressure as calculated from the radial flow bubble model (Ref. 8) has dropped to atmospheric by expansion. Prior to this time the water particles of the column top have moved upward ahead of the explosion product gases.

2 msec. The column has grown, but remains substantially the same shape. The tracer core has continued to move upward faster than the column top or crown and is now in the crown aerosol. At this depth the tracer reversal time as given in Fig. 4.2 is 3.5 msec; so that probably the tracer core is in contact with the crown aerosol for several milliseconds. During this short period, the Phase I tracer transfer must occur.

Actually, transfer of carbon particles from the explosion products to the crown must also occur during this period to a greater extent than the tracer, since the explosion products are probably distributed uniformly within the column. Photographs do not show the crown to be discolored with carbon at this time, indicating that the carbon is not transferred to the outside droplets of the crown.

The underwater bubble or cavity continues to grow rapidly as a result of the kinetic energy delivered to the surrounding water during the initial explosion product gas expansion, thus increasing the volume within the column walls and bubble and dropping the internal pressure well below atmospheric. This pressure differential is the major force which results in the downward reversal of the explosion products and tracer core.

5 msec. The column continues to grow both in diameter and height, with the crown becoming more broad and well defined. The bubble and column cavity have grown further, thus resulting in an even greater reduction of the internal pressure below atmospheric.

C O N F I D E N T I A L

The tracer core has now reversed downward and is just below the crown. However a small fraction of this tracer is shown to have been transferred to the water particles at the crown center. This phase I transfer must occur by this time to explain the subsequent tracer distribution in the crown at 27 msec. Possible inward flow of air from the top of the column is indicated by arrows. Such a counter flow of air opposing the upward motion of the water particles in the crown may be partly responsible for the characteristic broad crown formation.

10 msec. The crown column and bubble have again grown larger, and the crown is now well developed. Excursion of the tracer core is now nearly complete, with the bulk of the tracer about to return to the bubble. Some smearing of the tracer along the vertical axis is evident from the radiation detector data. The tracer distribution data requires some means of accounting for radial distribution of the tracer fraction transferred to the crown; so dashed arrows have been used to indicate the circulation within the crown.

20 msec. This is a time of sharp transition between both hydrodynamic and tracer transfer phases; consequently, conditions cannot be precisely defined. Some features are readily apparent. The column walls are now vertical rather than acute. The tracer has returned to the bubble and is probably mixing with the explosion products, and the column walls are still flowing upward. Other more speculative features are shown with dashed lines and include the actual position of the interior column walls, formation of the downward jet, and the remnant of the smeared tracer core within the column. The downward jet formation is discussed at length in Refs. 1 and 8 and consists of both water and air flowing in from the column top. The column walls are in the process of converging to form a central upward jet, as is shown in the following figure (40 msec). This convergence results from the differential pressure across the column walls. The exact stage of formation of the

C O N F I D E N T I A L

downward jet which is associated with bubble top period is uncertain. However it is shown in dashed lines to indicate its formation which is completed in the next figure (40 msec).

40 msec. At this time, the crown is fully developed and the tracer transferred into it during Phase I has probably reached its final distribution. The upward flowing column walls have converged at about 6 to 8 ft, and the downward jet is protruding through the bottom of the bubble. The bubble, incidentally, is still growing, at least horizontally, and growth will continue until approximately 100 msec. The arrows indicate the direction of water flow from the column base into the column walls and downward jet as established in Ref. 1.

This is the start of Phase II transfer of tracer from the underwater bubble into the upward flowing column walls. The tracer that was returned to the bubble shortly after 10 msec has distributed itself within the bubble so as to allow transfer into the column walls. The details of the mixing process of the tracer after its return to the bubble are not known. However the downward jet may be an important mixing mechanism.

100 msec. At this time, the internal structure of the bubble and column are much the same as before, except that the upward and downward jets have extended. The Phase II transfer of tracer from the bubble is shown as having just ended. However the converging column walls and the central jet contain the tracer previously transferred. The existence of this second transfer mode into the column walls, and hence the jet, is clearly apparent from both the radiation measurements adjacent to the column and the tracer sampling data. Examination of radiation count rates for three detector heights given in Fig. 3.9, starting at about 20 msec, shows a broad secondary peak in each, occurring sequentially from the lowest to the highest detector level. This sequence of radiation peaks

C O N F I D E N T I A L

at successive detector heights can only be interpreted as the upward passage of a fraction of the tracer. Further, the tracer sampling data establishes that the tracer is transferred into the column walls and transported upward because the tracer radial distributions show the tracer sampled at later times to be associated with water of the central jet. This jet, of course, results from convergence of the column walls. No other mechanism is available to transport the tracer upward. In addition to the tracer transfer into the upward jet, it also is possible that tracer is transferred from the bubble to the downward jet.

700 msec. The third and final transfer phase takes place during the last hydrodynamic event, late emission or the collapse of the bubble cavity.^{7,11} As indicated previously, the bubble top, having a very short period, has completed its oscillation and formed the downward jet. However, the bubble bottom, having a longer period, collapses upward in the form of a blunt jet. The downward jet has had little or no disruptive effect on the bubble motion because during this period the bubble energy has been transferred to the surrounding water as kinetic and potential energy. The upward jet results, of course, when potential energy in the water is converted back into kinetic energy with a vertical component. The jet, consisting of water from beneath the bubble, moves rapidly upward smashing through the column walls and forcing the explosion products in the bubble to vent through the turbulent plumes. Since the plumes consist of heavy water spray, the opportunity is great for transfer of the explosion products and tracer into the plumes. The Phase III transfer of tracer is clearly apparent in the graph of count rate histories for the entire event shown in Appendix B-1. For the lowest detector height, the Phase III transfer period extends from 0.6 to 1.4 sec.

C O N F I D E N T I A L

C O N F I D E N T I A L

This period also may provide an opportunity for escape of the tracer fraction that is unaccounted for by the post-shot measurement of tracer remaining in the pond, as discussed previously. As the tracer and explosion products are forced out of the bubble cavity through the column walls and plumes by the late emission process, the opportunity for transfer into the water particles is great; however, the possibility of 10 % escaping as gas or very light aerosol is certainly reasonable. The fact that all of the tracer is accounted for in the pond water and that none escapes for charge depths of 5.5 in. or deeper is best explained by noting that the column walls are generally thinner as the detonation depth approaches the surface, thus providing less opportunity for transfer of the tracer into the water particles. The unaccounted-for fraction of tracer lost from the pond is thus most probably explained by this process.

A similar sequence of schematic drawings can be made for each of the other charge depths investigated. This was felt to be unnecessary because (1) the hydrodynamic processes do not significantly change for the other depths and (2) quantity of explosion product transfer is given for all depths elsewhere in the report.

APPLICATION OF RESULTS TO NUCLEAR PHENOMENA

The important question with respect to application of these findings to nuclear yields is whether the modes or phases of fission product transfer into the columns or crowns are similar to those which have been established for a traced one-pound yield. Transfer Phases I and III have been clearly associated with the top and bottom bubble motions, while Phase II is dependent on the upward flow of column walls and the distribution of the explosion products at the end of Phase I. For the shallow one-pound yield, the transfer phases were well separated in time because

C O N F I D E N T I A L

of the hydrodynamic sequence. However, bubble model calculations show that this sequence changes with yield. Therefore, the hydrodynamic processes are of most interest in the determination of the probable fission product transfer to be expected at the nuclear yields. As an aid to understanding the effects of increased yield on the hydrodynamic process, the period ratio of the bubble top and bottom vs. scaled depth computed from the bubble model is shown in Fig. 4.4. The relative period ratios are indicated for 3 yields: 1 lb, 10^4 lb, and 10 KT, along with the scaled depths of three pertinent nuclear test events. These curves have been computed by R. R. Hammond and presented in Ref. 2. The ratio of top to bottom bubble periods given by these curves is an indicator of the hydrodynamic sequence. When the ratio is less than one, the bubble top will jet downward through the bubble ahead of the bottom upward jet, and when the ratio is more than one, the bottom jet precedes the top.

Possibilities of fission product transfer to the columns and crowns by each of the three transfer modes will now be considered.

Phase I

As defined, transfer by the Phase I mode occurs as the fission product core moves upward into the column when the bubble top period is shorter than the bottom period. It has been shown that for one pound charges the return of the tracer to the below-surface bubble is associated with the top bubble period and such an excursion results in an initial radiation pulse. Examination of Fig. 4.4 will show that at shallow scaled depths all yields, including 10 KT, have a period ratio less than unity. Therefore the hydrodynamic conditions required for Phase I transfer are present. An initial radiation pulse, indicating an upward excursion of the fission products and thus Phase I transfer, has been observed at both nuclear tests and 10^4 -lb traced high explosive tests (Hydra IIA). In order to determine whether the initial radiation

C O N F I D E N T I A L

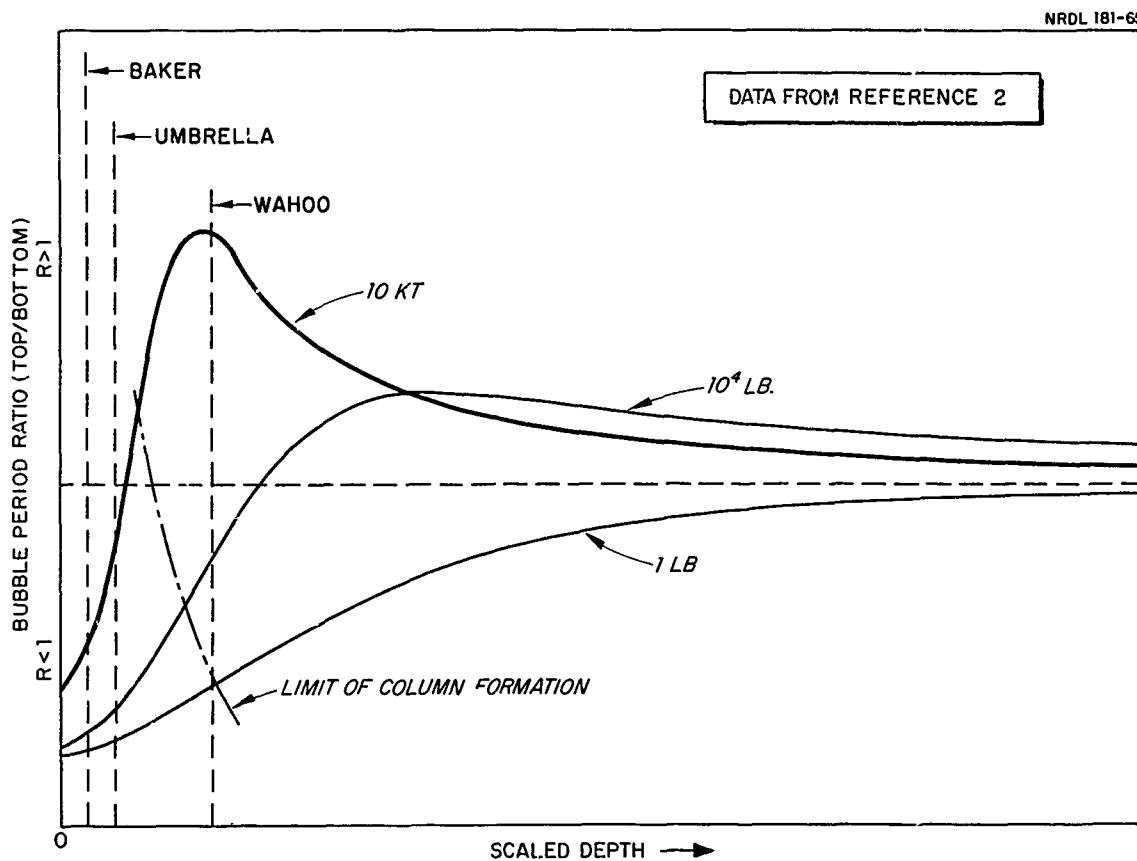


Fig. 4.4 Calculated Ratio of Bubble Top Period to Bubble Bottom Period vs. Scaled Depth for 1 lb, 10^4 lb and 10 KT yields

C O N F I D E N T I A L

pulses at the higher yields were also associated with the bubble top motion, the initial pulses from three yields (1 lb, 10^4 lb, and Umbrella) scaled to the Umbrella depth were time-scaled with the bubble top period predicted by the bubble model. The data used for 10^4 lb came from Ref. 7 and that for Umbrella from Ref. 12. The resulting scaled initial pulses are shown in Fig. 4.5 where the dose rate or count rate has been normalized and the time scaled by dividing the event times by the predicted bubble top period as indicated. The quite precise superposition of all three initial pulses demonstrates very clearly that an upward excursion of the fission products associated with the bubble top period occurs at the nuclear yield. It follows that Phase I transfer of fission products into the upper column also occurs.

Considerable effort was made to determine whether the scaled initial pulses could also be established at the scaled Baker depth. Unfortunately, none of the Baker test dose rate records were of high enough time resolution to see an initial radiation pulse. Also no data was available from the one traced Hydra IIA shot at this depth because of an instrument failure. Although it cannot be established directly for the nuclear yield at depths shallower than Umbrella, the one-pound results indicate that an initial fission product excursion, hence Phase I transfer, would be expected to shallow scaled depths at least half that of Baker (approximately 1.6 in. for 1 lb H.E.).

Phase II

The Phase II mode of fission product transfer into the column must occur after return of the fission products to the below-surface bubble and inclusion into the upward flowing column walls. The Phase II transfer depends on the existence of two conditions. The first condition is, of course, a detonation depth shallow enough so that column walls are formed. The formation of column walls is independent of the bubble top

C O N F I D E N T I A L - FORMERLY RESTRICTED DATA

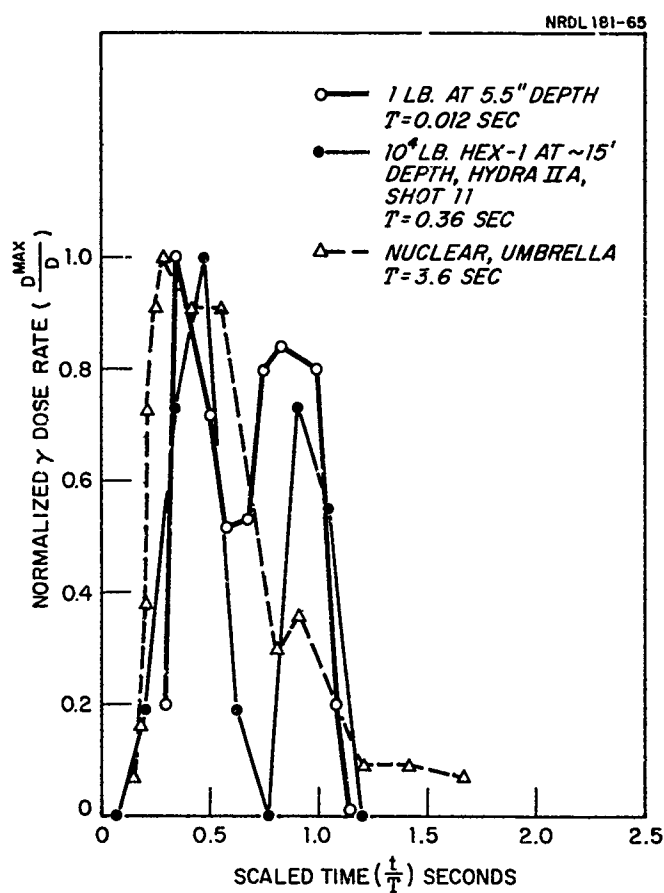


Fig. 4.5 Initial Gamma Pulse From 1 lb, 10^4 lb and Nuclear Yields Time-Scaled With Calculated Bubble-Top Period

C O N F I D E N T I A L -
FORMERLY RESTRICTED DATA

or bottom oscillation and probably also of yield. Column walls would be expected to detonation depths of about half the maximum bubble radius. A curve for the limit of column formation is given in Fig. 4.4. This limit is not at constant scaled depth for the yields given because it is based on constant geometry rather than conventional $(D/w^{1/3})$ scaled depths.

The second condition required for Phase II transfer is a mechanism for dispersion of the fission products from the initial central concentration to the outer bubble surfaces and hence into the column walls. It should be pointed out here that the fission products have been predicted to be centrally concentrated during the first bubble expansion by Snay,⁹ and this has been verified experimentally with exploding wires.¹⁰ The mixing or dispersion of the fission products very probably depends on the action of the bubble top as it jets downward through the bubble. The downward jet can occur only for scaled depths where the bubble top to bottom period ratios is less than unity. Obviously for conditions where the top and bottom bubble periods are equal, reduced mixing would be expected and hence little chance for Phase II transfer. Thus, the hydrodynamic conditions for Phase II transfer of fission products into the column walls are limited to shallow depths where column walls are formed and shorter top bubble period provides fission product mixing. For 10-KT nuclear underwater explosions, Fig. 4.4 shows that the Umbrella-scaled depth is about the lower limit for Phase II transfer.

Phase III

The Phase III mode of fission product transfer occurs as the bubble bottom collapses upward, forcing all the remaining fission products in the bubble into the plumes. This transfer phase can occur either as the third phase for shallow depths (the plumes are commonly referred to as late emission) or as the only mode of transfer for deeper detonation

depths where no column forms. Considering the shallow condition at nuclear yields, some important differences are apparent from Fig. 4.4. The most significant difference is that for increasing yield, the bubble period ratio (top to bottom) approaches unity for shallow depths, where columns are formed, with the result that the bubble bottom period is only slightly longer than the top period. The conditions for Phase II transfer are present, and it is possibly under-way, but it is prematurely terminated by the almost immediate onset of upward bubble bottom collapse as Phase III mode disrupts the column walls. Thus, for nuclear yields at shallow depths, the Phase III transfer mode might be expected to preempt the Phase II mode and become the dominant mode of fission product transfer.

Considering now the deep depth condition where no column walls are formed, the Phase III mode of fission product transfer becomes the only one possible because the bubble bottom period is very much shorter than the top period. Referring to Fig. 4.4, the bubble period ratio for 10 KT yield is seen to maximize at the Wahoo-scaled depth. This would imply that hydrodynamically the conditions are optimum for Phase III transfer of fission products into the plumes, because the bubble bottom jet would most likely have maximum energy and velocity when it smashes into the water layer over the bubble top. Admittedly, the Phase III mode differs somewhat from shallow to deep depths in that the bottom jet encounters a different fission product distribution within the bubble and column walls rather than an overlying water layer. However, it seems justifiable to consider it as one process because it results at both depths from the bubble bottom motion. As the depth increases, the bubble period ratio decreases, and a depth is soon reached where the bottom jet cannot penetrate the water overlayer so that the bubble must oscillate through another period. On the next oscillation the bubble bottom will again have a shorter period. If sufficient upward migration has occurred, the bottom jet will penetrate the surface and result in plumes with Phase III fission product transfer.

C O N F I D E N T I A L

This fission product transfer mode is of major importance because it provides the mechanism for base surge aerosol generation and contamination with fission products. For the deep depths it is the only mechanism available, but for shallow depths subsidence of the column walls provides an additional mechanism. In order for subsidence of the column walls to be a prominent mechanism for generation of a contaminated base surge, a large fraction of the fission products would have to transfer into the walls via the Phase II mode. Considering the relatively small fraction of tracer transferred via Phase II (which has been established earlier in this report), the major base surge generation and contamination mechanism for shallow detonations must also be associated with the Phase III mode.

SHALLOW BOTTOM EFFECTS

All the experimental and analytical results of this report have considered the underwater explosion to be unaffected by proximity to a shallow bottom. Actually, for nuclear application to nuclear test data, this is unrealistic because both Baker and Umbrella were fired on or near a shallow bottom. Since it has been shown that fission product transfer is clearly dependent on the hydrodynamic processes, some consideration of shallow bottom effects on the hydrodynamic processes and hence on the transfer processes seems in order. Comments will be made on the possible effects for each transfer phase. However, these are only speculations because no experimental data is available and the bubble model has not been extended to the shallow bottom condition.

Considering Phase I transfer first, a large increase in the total fraction of fission products transferred into the crown might be expected. There are two effects which would tend to promote this increase. The first effect would be an increase in the height within the column of the

C O N F I D E N T I A L

C O N F I D E N T I A L

fission product core excursion because of the restricted expansion volume for the lower part of the bubble. The gas expands above the surface with the fission product core approximately centered because of the higher resistance of the water below; so any additional resistance would be expected to increase the amplitude of the excursion. The other effect would be a slower period for the excursion of the fission product core within the column, since the period is a function of the bubble pressure which would not drop so quickly with restricted expansion of the bubble bottom. Note that this period change did not show up in the scaled initial pulse for shot Umbrella given in Fig. 4.5. However, this does not exclude the possibility for shallower depths. Both of these effects would allow the fission product core an enhanced opportunity for transfer into the water particles of the column crown.

The probable effects on Phase II transfer into the column walls is not apparent. The transfer is dependent on dispersion of the fission products within the bubble, via a process which is not understood for the bottom free case. Speculation as to changes of this dispersion or mixing process, when the bubble shape has been changed from a hemisphere to a flat disk, seems of little value. It will suffice to say that the effects on Phase II transfer due to a shallow bottom are not now predictable. It will be pointed out that evidence from H. E. tests indicates the column-formation mechanisms to be unchanged by a shallow bottom.

The shallow bottom would be expected to cause a considerable reduction of Phase III transfer to the late emission plumes and hence into the base surge. This mode of transfer normally occurs as the result of the upward jetting of the bubble bottom, but the shallow bottom now alters the process to a radial inward collapse of the cavity sides. The radial collapse of the sides would be expected to result finally in an upward jet; however, both its period and energy would be changed. The period would be longer and probably near that of the bubble side, so that less chance

C O N F I D E N T I A L

for interference with Phase II transfer might be expected. The energy of the final jet would be severely reduced because of losses to bottom friction and, more important, to bottom cratering. With a less energetic final jet it is reasonable to expect less energetic interaction with the column and possibly less fission product transfer into the base surge.

The probable net effect of a shallow bottom is then to shift a larger fraction of the fission products into the upper column or crown via Phase I transfer, and reduce the Phase III transfer with its resulting effect on the base surge.

Note. This document is classified CONFIDENTIAL - FORMERLY RESTRICTED DATA, Group I, based on the classified yield revealed on pages 57, 59, 60, and 61. All other information is unclassified.

C O N F I D E N T I A L

C O N F I D E N T I A L

CONCLUSIONS

The following conclusions may be drawn from this investigation with small, H.E., traced charges and from analysis of the results with some nuclear test data:

(a) Three modes of fission or explosion product transfer from the explosion bubble into the above-surface columns and plumes have been established for shallow underwater explosions.

(b) The three fission product transfer phases are dependent on the hydrodynamic processes involving column formation and the motions of the upper and lower portions of the explosion bubble.

(c) A modified form of the radial flow bubble model, which predicts the independent motions of the top and bottom of the explosion bubble for yields up to the nuclear range, can be employed to predict the expected fission product transfer modes at specific yield and depth conditions.

(d) The fraction of fission products transferred into crown and column of near surface and very shallow underwater detonations in deep water is approximately 5 % and 4 % respectively. However, virtually no transfer into the column occurs at detonation depths scaled to the Umbrella nuclear event or deeper.

(e) A shallow bottom condition might be expected to result in hydrodynamic changes and, consequently, differences in the modes of fission

C O N F I D E N T I A L

C O N F I D E N T I A L

product transfer from deep water conditions. For shallow bottom nuclear detonations, the expected effect relative to a deep bottom condition (with the same charge depth) is increased transfer of fission products to the column and crown, but decreased transfer into a less prominent base surge. Therefore serious errors are possible when radiological predictions are made for shallow nuclear explosions in deep water that are based on test results from shallow bottom shots such as Baker and Umbrella.

C O N F I D E N T I A L

C O N F I D E N T I A L

REFERENCES

1. K. W. Kaulum, "Hydra IIB Series - Investigation by Water Sampling of the Internal Structure of Columns Resulting From Small Underwater Explosions," USNRDL-TR-706, Sept. 1963 (UNCLASSIFIED).
2. R. R. Hammond, "Hydra IIA-B Series - An Investigation of Water Flow Adjacent to Underwater Explosion Bubbles Using Fluorescent Dyes and Photographic Techniques (U)," USNRDL-TR- (UNCLASSIFIED).
3. W. E. Strobe, "Investigation of Gamma Radiation Hazards Incident to an Underwater Atomic Explosion (U)," USNRDL-TR-687, 5 Nov. 1963 (CONFIDENTIAL).
4. E. C. Evans, III, T. H. Shirasawa, "Characteristics of the Radioactive Cloud From Underwater Bursts, Project 2.3, Operation Hardtack (U)," U. S. Naval Radiological Defense Laboratory WT-1621, 15 Jan. 1962 (CONFIDENTIAL). Published by Defense Atomic Support Agency.
5. R. L. Stetson, et al. "Radiological Capabilities of Nuclear Weapons as Determined by High Explosive Models, I. Shallow Underwater Studies," USNRDL-TR-17, 15 Oct. 1954 (UNCLASSIFIED).
6. J. W. Hendricks, D. L. Smith, "Above and Below Surface Effects of One-Pound Underwater Explosions, Hydra I," USNRDL-TR-480, 18 Oct. 1960 (UNCLASSIFIED).
7. W. J. Gurney, P. A. Killeen, "Hydra Program, Hydra IIA Series - Distribution of Explosion Products in the Above-Surface Phenomena of Very Shallow and Shallow Underwater Explosions (U)," USNRDL-TR-785, 6 July 1964 (CONFIDENTIAL).
8. R. R. Hammond, F. H. Young, E. A. Schuert, "Bubble Hydrodynamics of Shallow Underwater Explosions (U)," Proceedings of the Sixth Navy Sciences Symposium, Vol. II, ONR-12, May 1962 (CONFIDENTIAL).
9. H. G. Snay, "The Hydrodynamic Background of the Radiological Effects of Underwater Nuclear Explosions (U)," Proceedings of the Tripartite Symposium on Technical Status of Radiological Defense in the Fleets, Vol. II. USNRDL-R&L No. 103, 20 May 1960 (CONFIDENTIAL).
10. R. R. Buntzen, "The Underwater Distribution of Explosion Products From a Submerged Exploding Wire," USNRDL-TR-778, 31 July 1964 (UNCLASSIFIED).

C O N F I D E N T I A L

11. W. W. Perkins, "Hydra Program, Hydra IIA Series - The Above Surface Phenomena Created by 10,000-Pound Underwater Detonations (U)," USNRDL-TR-708, 28 October 1963 (CONFIDENTIAL).
12. M. M. Bigger, et al, "Shipboard Radiation From Underwater Bursts (U)," WT-1619, 24 March 1961 (CONFIDENTIAL). Published by Defense Atomic Support Agency.

C O N F I D E N T I A L

C O N F I D E N T I A L

APPENDIX A

RADIAL DISTRIBUTIONS OF CUMULATIVE WATER SAMPLE VOLUME AND TOTAL EJECTED
WATER VOLUME

C O N F I D E N T I A L

C O N F I D E N T I A L

TABLE A.1

Charge Depth = 1.6 in.

Time (ms)	Sample Volume (ml)							
	Sampling Radius (in.)							
	0	6	12	18	24	30	36	42
<u>$h_s = 92.5$ in. (8 ft)</u>								
27	T	T	T	T	T	T	T	T
52	160	70	4	1	T	T	T	T
100	305	70	4	1	T	T	T	T
300	746	70	4	1	T	T	T	T
<u>$h_s = 128.5$ in. (11 ft)</u>								
100	223	17	1	T	T	T	T	T
	405	61	4	T	T	T	T	T
T = trace; volume less than 1ml								

C O N F I D E N T I A L

TABLE A.2

Charge Depth = 2.5 in.

Time (ms)	Sample Volume (ms)							
	Sampling Radius (in.)							
	0	6	12	18	24	30	36	42
<u>$h_s = 68.5$ in. (6 ft)</u>								
100	229	22	7	1	2	T	0	0
300	340	63	4	2	T	0	0	
<u>$h_s = 92.5$ in. (8 ft)</u>								
27	2	T	T	T	T	T	T	T
52	139	10	2	T	T	T	T	T
100	305	20	2	T	T	T	T	T
300 +	927	54	6	T	T	T	T	T
<u>$h_s = 128.5$ in. (11 ft)</u>								
27	T	T	T	T	T	T	T	0
52	53	5	T	T	T	T	T	0
100	232	34	1	T	T	T	T	0
300	746	52	7	T	T	T	T	0

T = trace; volume less than 1 ml

C O N F I D E N T I A L

TABLE A.3

Charge Depth = 3.5 in.

Time (ms)	Sample Volume (ml)							
	Sampling Radius (in.)							
	0	6	12	18	24	30	36	42
$h_s = 68.5 \text{ in. (6 ft)}$								
50	105	8	4	3	1	T	T	0
100	213	28	8	3	1	T	T	0
300	437	102	8	5	3	2	T	0
$h_s = 128.5 \text{ in. (11 ft)}$								
100	270	18	2	T	T	T	T	T
300	-	88	5	T	T	T	T	T

T = Trace; volume less than 1 ml

C O N F I D E N T I A L

TABLE A.4

Charge Depth = 5.5 in.

Time (ms)	Sample Volume (ml)							
	Sampling Radius (in.)							
	0	6	12	18	24	30	36	42
<u>$h_g = 68.5$ in. (6 ft)</u>								
50	22	3	3	4	6	4	T	T
100	158	24	9	9	9	5	2	T
200	258	67	15	9	5	5	2	T
	330	153	15	9	9	5	2	T

T = trace; volume less than 1 ml

C O N F I D E N T I A L

TABLE A.5

Charge Depth = 7.5 in.

Time (ms)	Sampling Volume (ml)							
	Sampling Radius (in.)							
	0	6	12	18	24	30	36	42
<u>$h_g = 68.5$ in. (6 ft)</u>								
100	132	17	10	11	10	6	1	T
300 +	314	21	15	11	10	6	1	T
<u>$h_g = 63.5$ in. (6 ft)</u>								
100	76	32	23	23	17	10	5	2
200	204	53	23	23	17	10	5	2
300 +	321	175	32	23	17	10	5	2
T = trace; volume less than 1 ml								

C O N F I D E N T I A L

TABLE A.6
Total Ejected Water (liters)

Charge Depth (in.)	Sampling Height (in.)	Sampling Termination Time (msec)											Total Event
		12	17	22	27	32	52	100	200	300	500	700	
1.6	92.5				6.1		61.3	70.6		93.7			66.8
1.6	128.5							29.8					
2.5	20.5	(11.3)	(47.2)		(52.2)					(214)			(431)
2.5	68.5							41.0		(78)			(78)
2.5	92.5				6.2		21.8	37.3		98.0			98.0
2.5	128.5				6.1		12.4	38.6		86.3			
3.5	68.5						23.5	47.1		108.2			
3.5	128.5							34.7					
5.5	20.5		(48.0*)				(183)	(297)	(323)	(328)	(364)	(392)	(644)
5.5	44.5												(145)
5.5	68.5						34.5	82.8	118.0	147.8			166.7
5.5	72.5												(153)
7.5	20.5		(51.8**)							(419)			(600)
7.5	68.5							84.2		200.1			200.1
12	20.5			(80.5***)			(257)	(384)		(405)	(425)		(947)
12	44.5												(230)
12	68.5							160.0	178.7	258.2			258.2
24	20.5					(122)				(354)			(678)
24	68.5									(314)			(396)

* Actual $d_c = 4.5$ in.
** Actual $d_c = 6.5$ in.
***Actual $d_c = 10.75$ in.

NOTES: (1) Values in parentheses are unchanged from previous Ref. 1.
(2) Values underlined have been revised from those reported in Ref. 1.
(3) Unmarked values are new data.

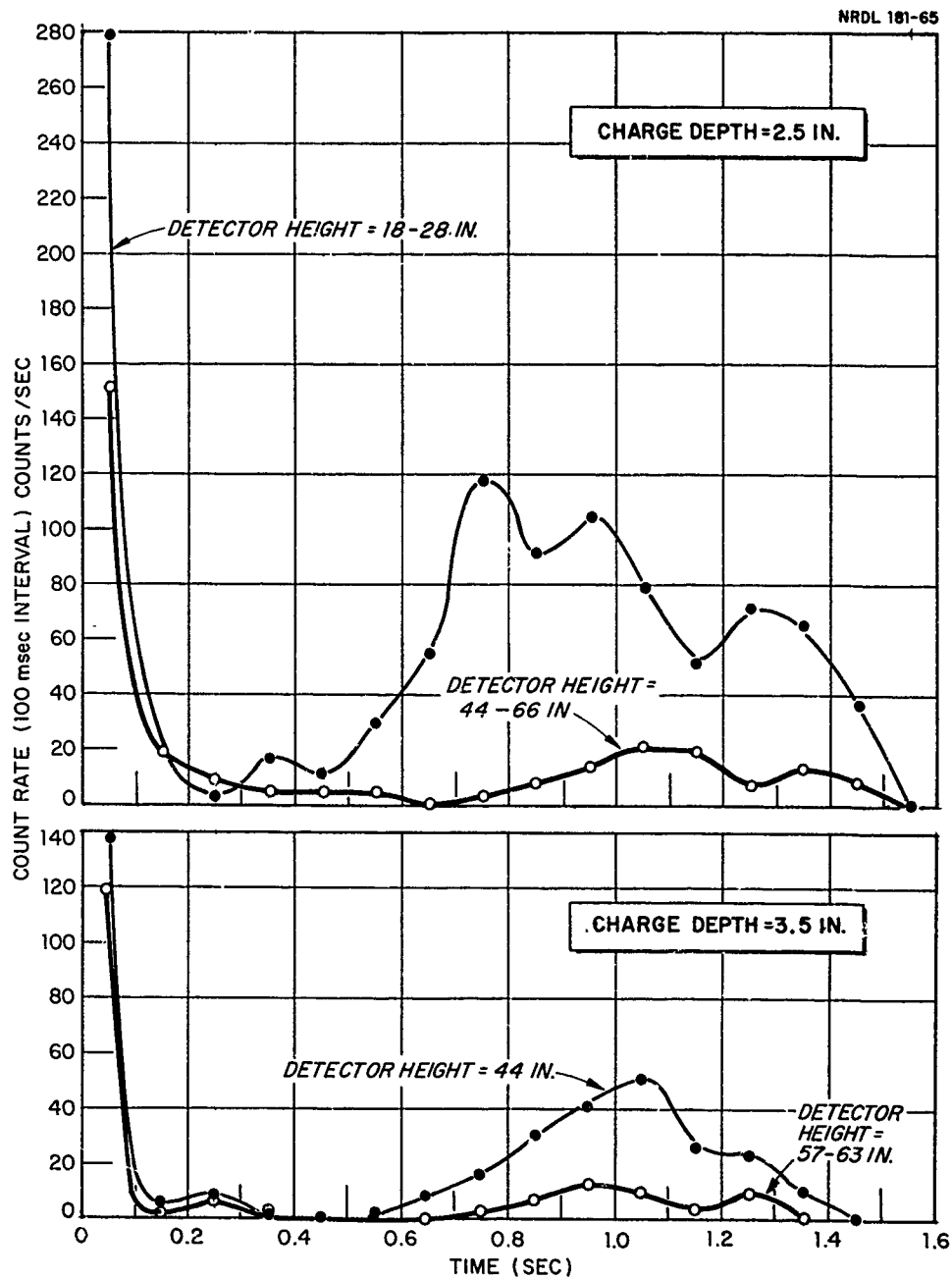
C O N F I D E N T I A L

APPENDIX B

GAMMA DETECTOR COUNT RATE (100 msec interval) ADJACENT TO THE COLUMN
FOR CHARGE DEPTHS OF 2.5, 3.5, 5.5, 7.5 AND 12 IN.

C O N F I D E N T I A L

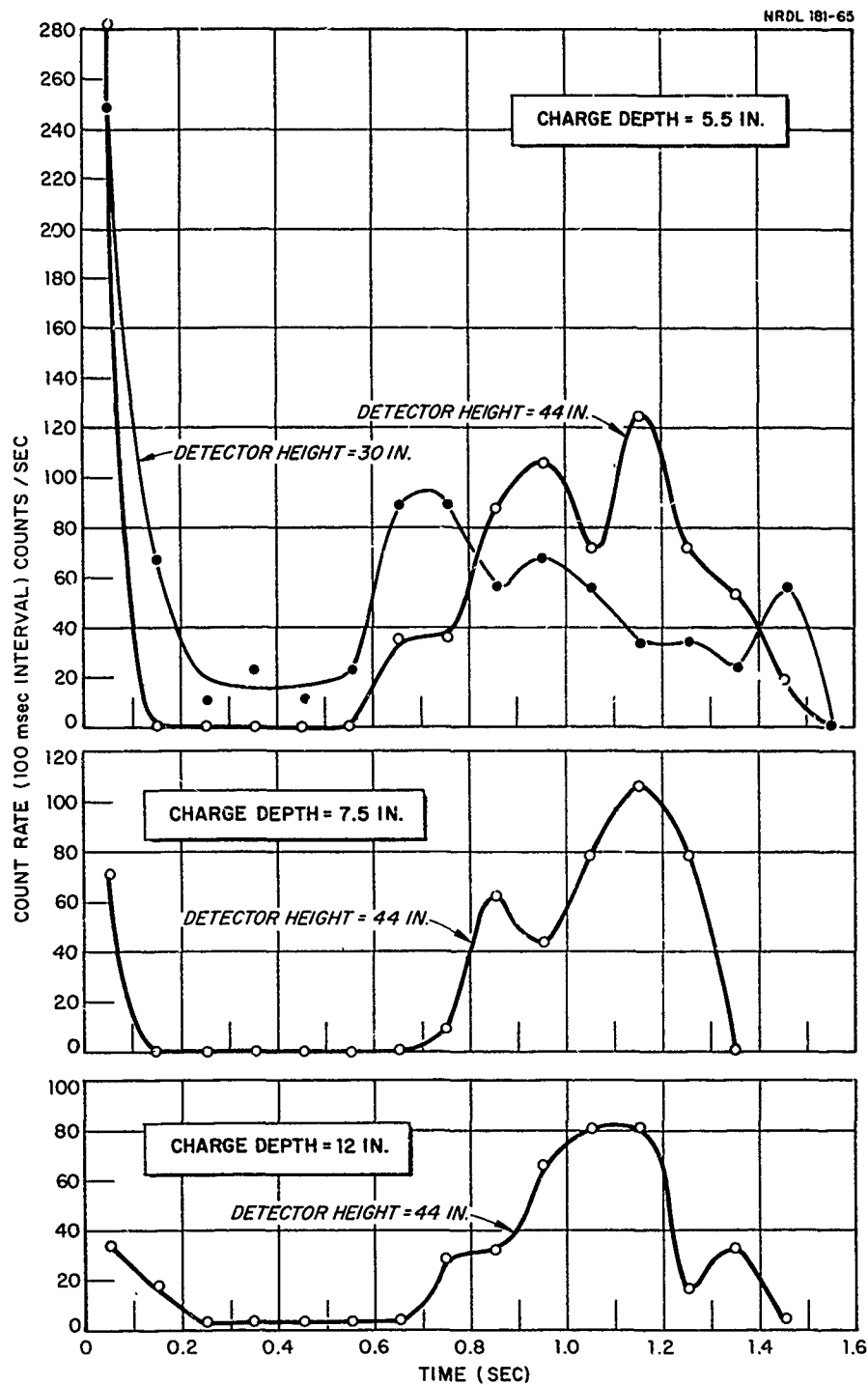
C O N F I D E N T I A L



Figs. B.1 and B.2

C O N F I D E N T I A L

C O N F I D E N T I A L



Figs. B.3, B.4 and B.5

C O N F I D E N T I A L

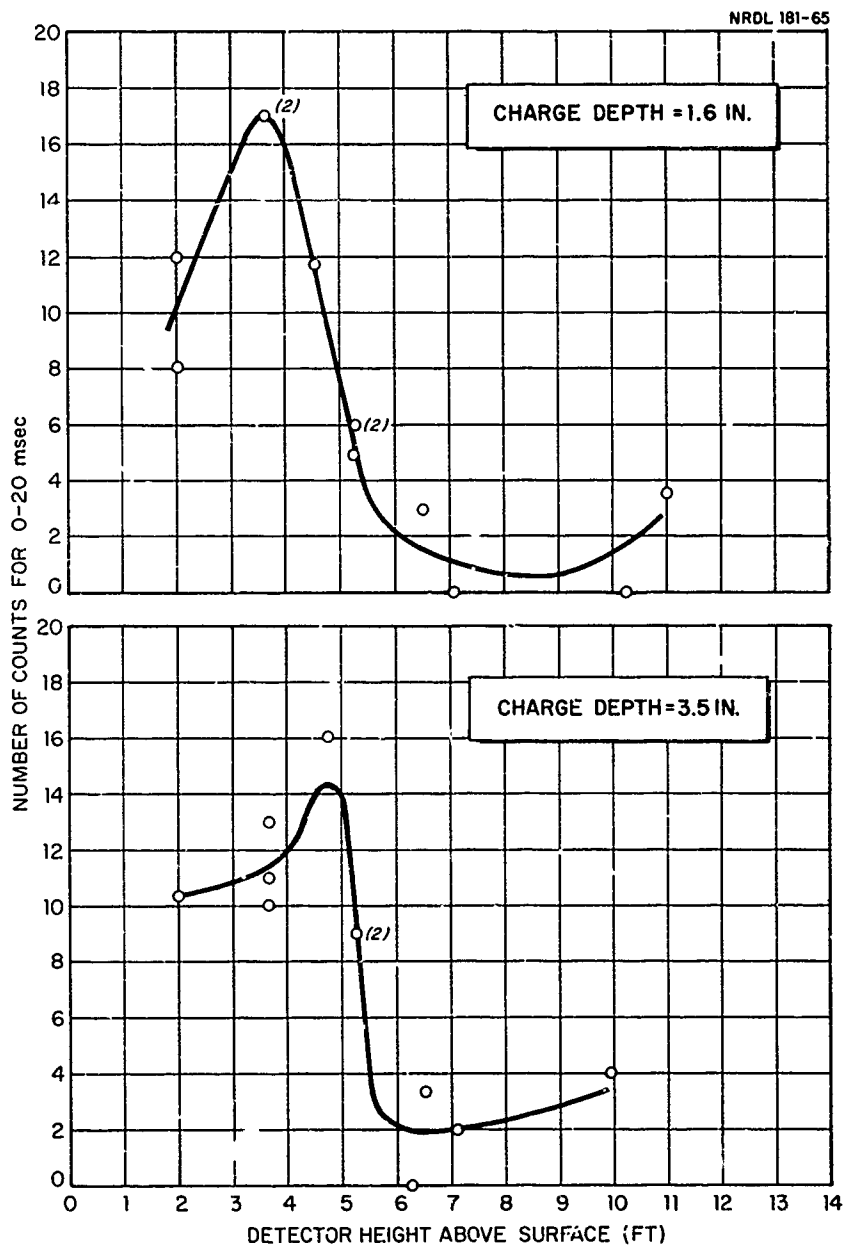
C O N F I D E N T I A L

APPENDIX C

NUMBER OF COUNTS FROM THE GAMMA DETECTOR DURING THE FIRST 20 MSEC
VS. DETECTOR HEIGHT FOR CHARGE DEPTHS OF 1.6 AND 3.5 IN.

C O N F I D E N T I A L

C O N F I D E N T I A L



Figs. C.1 and C.2

C O N F I D E N T I A L

C O N F I D E N T I A L

APPENDIX D

HIGH RESOLUTION INITIAL COUNT RATE AT VARIOUS GAMMA DETECTOR HEIGHTS VS.
TIME FOR CHARGE DEPTHS 1.6 TO 7.5 IN.

NOTE: The 3 graphs in Fig.D-1 show the data for each detector height at 2.5 in. charge depth which were combined to make Fig. 3.9 in the main text. The remaining graphs show only the combined curves for charge depths of 1.6, 3.5, 5.5 and 7.5 in.

C O N F I D E N T I A L

C O N F I D E N T I A L

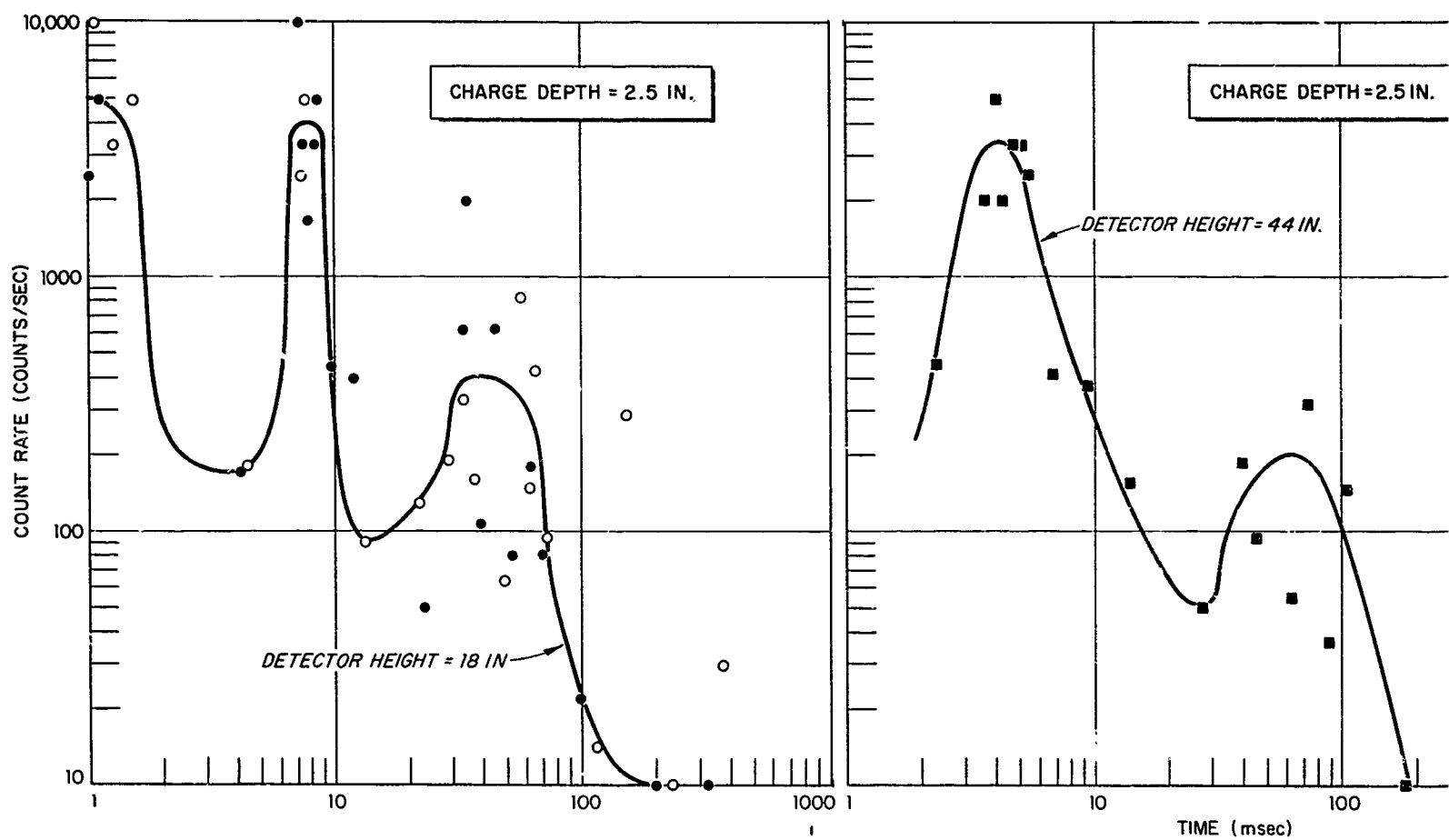


Fig. D.1

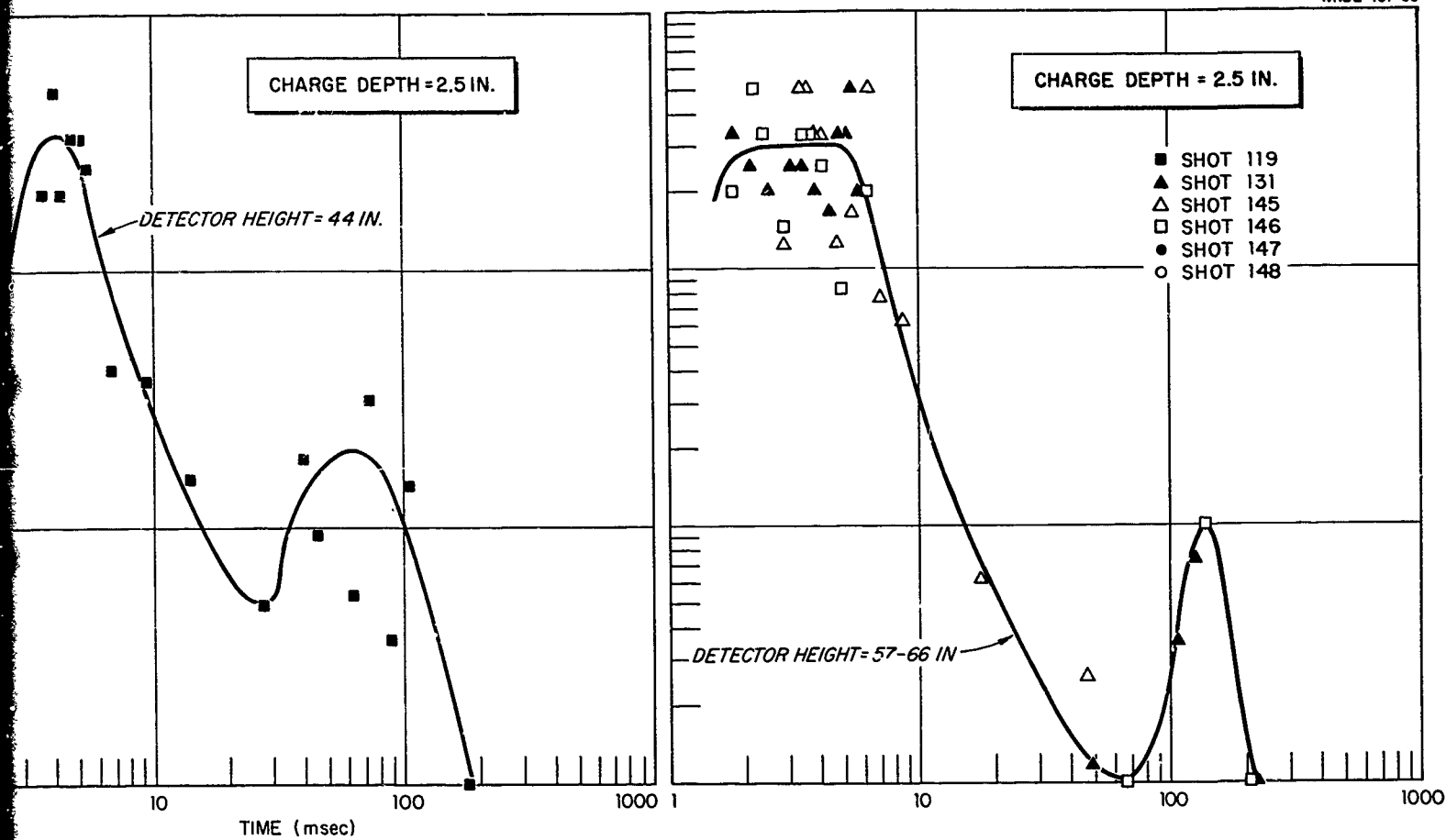


Fig. D.1

C O N F I D E N T I A L

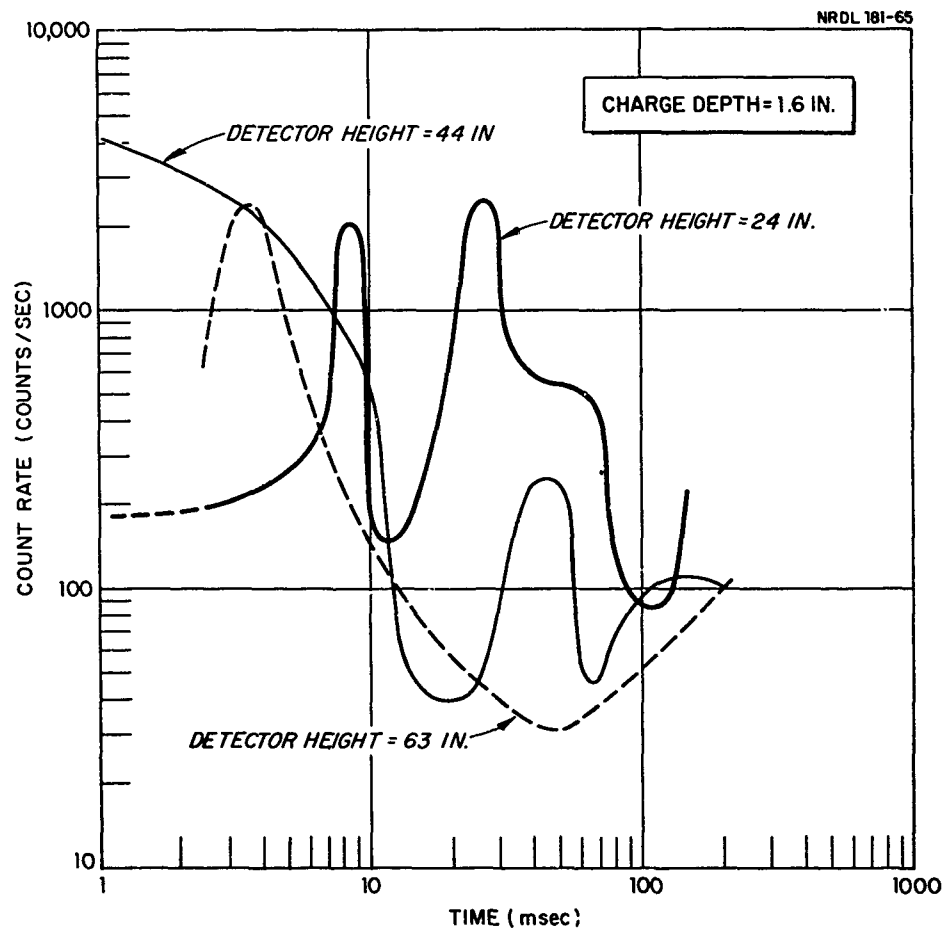


Fig. D.2

C O N F I D E N T I A L

C O N F I D E N T I A L

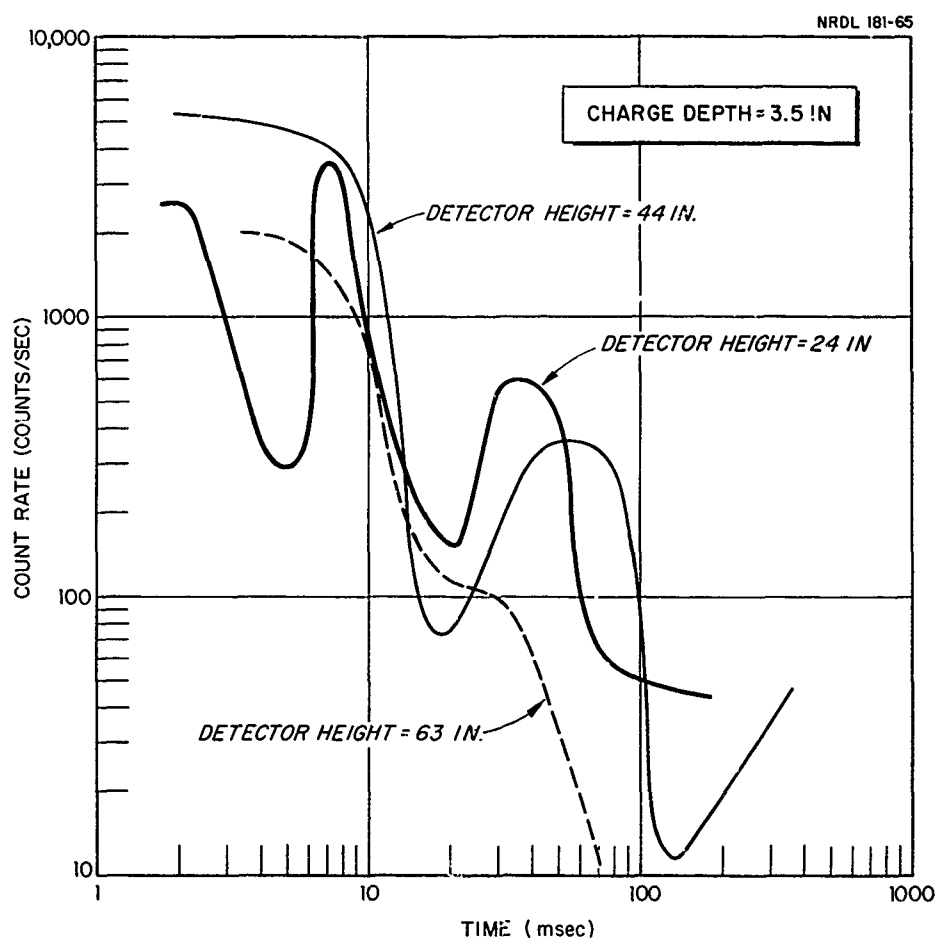


Fig. D.3

C O N F I D E N T I A L

C O N F I D E N T I A L

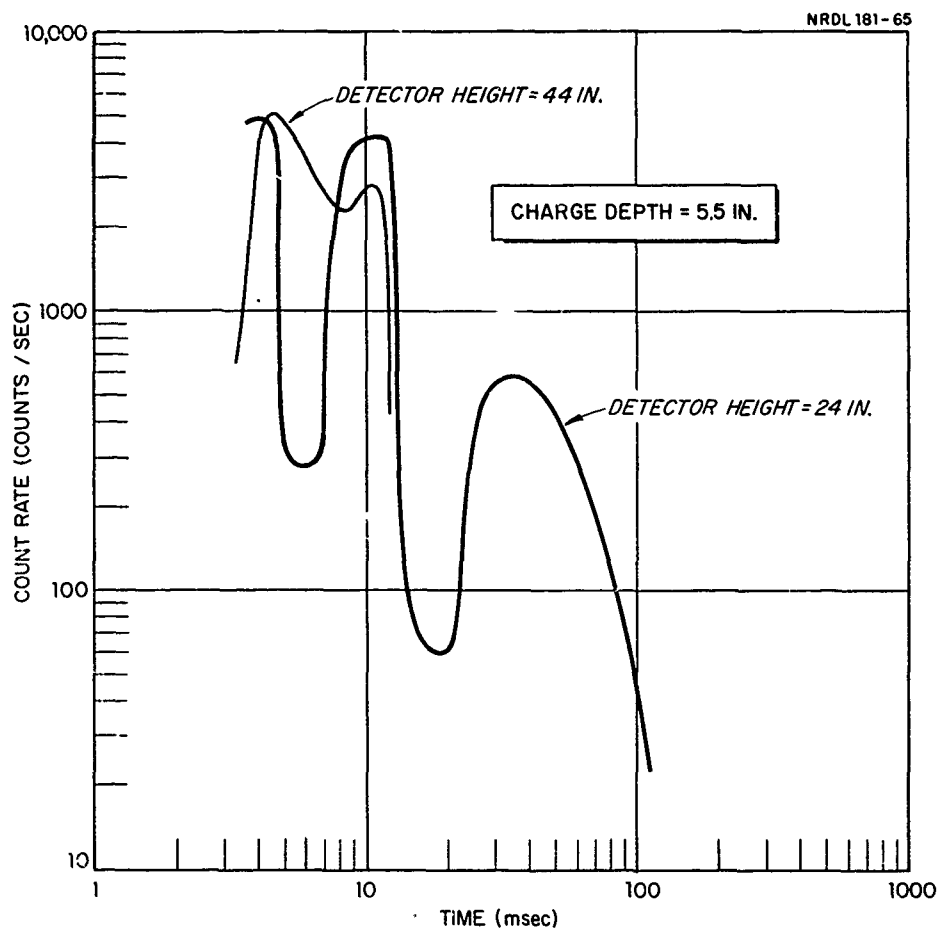


Fig. D.4

C O N F I D E N T I A L

C O N F I D E N T I A L

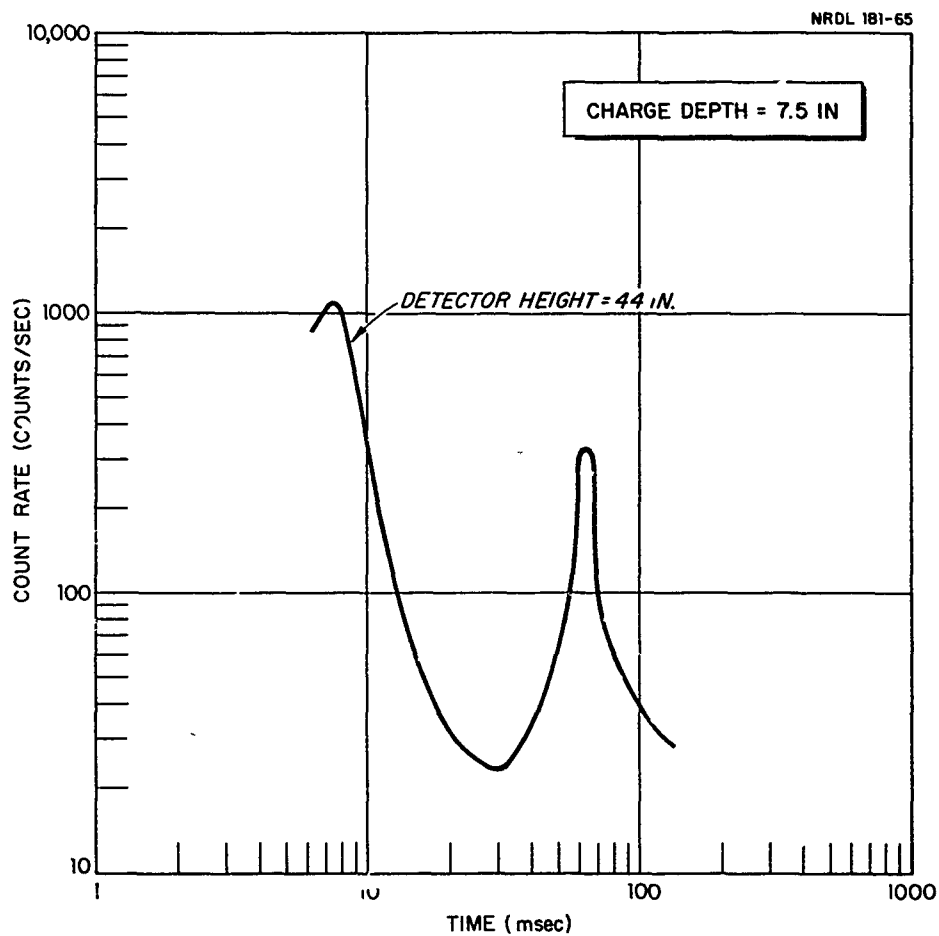


Fig. D.5

C O N F I D E N T I A L

<p>Naval Radiological Defense Laboratory USNRDL-TR-954 (DASA-1726) HYDRA PROGRAM. HYDRA IIB SERIES - TRANSFER AND DISTRIBUTION OF TRACED EXPLO- SION PRODUCTS TO THE COLUMNS OF SHALLOW UNDERWATER EXPLOSIONS (U), by K. W. Kaulum 30 September 1965 100 p. tables illus. 12 refs. CONFIDENTIAL FORMERLY RESTRICTED DATA</p> <p>The transfer of explosion products into the above-surface column and crown of a shallow underwater explosion was investigat- ed with traced (Au198) one-pound spherical pentolite charges fired at depths of 1.6 to 7.5 in. Tracer transfer data was obtained (over)</p> <p>I. Kaulum, K. W. II. Title III.</p> <p>Abstract UNCLASSIFIED</p>	<p>1. Underwater explo- sions 2. Explosion bubbles 3. Nuclear explosions 4. Hydrodynamics 5. Explosion effects, Underwater-to-air</p>
<p>Naval Radiological Defense Laboratory USNRDL-TR-954 (DASA-1726) HYDRA PROGRAM. HYDRA IIB SERIES - TRANSFER AND DISTRIBUTION OF TRACED EXPLO- SION PRODUCTS TO THE COLUMNS OF SHALLOW UNDERWATER EXPLOSIONS (U), by K. W. Kaulum 30 September 1965 100 p. tables illus. 12 refs. CONFIDENTIAL FORMERLY RESTRICTED DATA</p> <p>The transfer of explosion products into the above-surface column and crown of a shallow underwater explosion was investigat- ed with traced (Au198) one-pound spherical pentolite charges fired at depths of 1.6 to 7.5 in. Tracer transfer data was obtained (over)</p> <p>I. Kaulum, K. W. II. Title III.</p> <p>Abstract UNCLASSIFIED</p>	<p>1. Underwater explo- sions 2. Explosion bubbles 3. Nuclear explosions 4. Hydrodynamics 5. Explosion effects, Underwater-to-air</p>

both by water sampling within the columns and radiation measurements adjacent to the columns. Radial tracer distributions in the column were integrated to give the total fraction of tracer transferred into the column as a function of time. A maximum of 5% of the tracer was transferred into the column at the shallowest charge depth. Data analysis has established three distinct modes of tracer transfer into the above-surface columns or plumes which are shown to be associated with hydrodynamic processes involving the column, or the explosion product bubble. The results are applied to full scale nuclear yields by utilizing a modified radial flow bubble model as a means of predicting the expected fission product transfer modes for specific nuclear yield and depth conditions.

Abstract
UNCLASSIFIED

both by water sampling within the columns and radiation measurements adjacent to the columns. Radial tracer distributions in the column were integrated to give the total fraction of tracer transferred into the column as a function of time. A maximum of 5% of the tracer was transferred into the column at the shallowest charge depth. Data analysis has established three distinct modes of tracer transfer into the above-surface columns or plumes which are shown to be associated with hydrodynamic processes involving the column or the explosion product bubble. The results are applied to full scale nuclear yields by utilizing a modified radial flow bubble model as a means of predicting the expected fission product transfer modes for specific nuclear yield and depth conditions.

Abstract
UNCLASSIFIED

UNCLASSIFIED

Security Classification

DOCUMENT CONTROL DATA - R&D		
(Security classification of title, body of abstract and indexing annotation must be entered when the overall report is classified)		
1. ORIGINATING ACTIVITY (Corporate author) U. S. Naval Radiological Defense Laboratory San Francisco, California 94135		2a. REPORT SECURITY CLASSIFICATION CONFIDENTIAL - FRD 2b. GROUP 1: Downgraded at 3 yr intervals; declassified after 12 years.
3. REPORT TITLE HYDRA PROGRAM. HYDRA IIB SERIES - TRANSFER AND DISTRIBUTION OF TRACED EXPLOSION PRODUCTS TO THE COLUMNS OF SHALLOW UNDERWATER EXPLOSIONS (U)		
4. DESCRIPTIVE NOTES (Type of report and inclusive dates)		
5. AUTHOR(S) (Last name, first name, initial) Kaulum, Keith W.		
6. REPORT DATE 5 April 1966	7a. TOTAL NO. OF PAGES 100	7b. NO. OF REFS 12
8a. CONTRACT OR GRANT NO. b. PROJECT NO NWER Program A-7, Subtask 10.002 c d		9a. ORIGINATOR'S REPORT NUMBER(S) USNRDL-TR-954 9b. OTHER REPORT NO(S) (Any other numbers that may be assigned this report) DASA-1726
10. AVAILABILITY/LIMITATION NOTICES U. S. Military Agencies may obtain copies of this report directly from DDC. Other qualified users should request through Director, DASA.		
11. SUPPLEMENTARY NOTES		12. SPONSORING MILITARY ACTIVITY Defense Atomic Support Agency Department of Defense Washington, D. C. 20301
13. ABSTRACT The transfer of explosion products into the above-surface column and crown of a shallow underwater explosion was investigated with traced (Au^{198}) one-pound spherical pentolite charges fired at depths of 1.6 to 7.5 in. Tracer transfer data was obtained both by water sampling within the columns and radiation measurements adjacent to the columns. Radial tracer distributions in the column were integrated to give the total fraction of tracer transferred into the column as a function of time. A maximum of 5% of the tracer was transferred into the column at the shallowest charge depth. Data analysis has established three distinct modes of tracer transfer into the above-surface columns or plumes which are shown to be associated with hydrodynamic processes involving the column or the explosion product bubble. The results are applied to full scale nuclear yields by utilizing a modified radial flow bubble model as a means of predicting the expected fission product transfer modes for specific nuclear yield and depth conditions. (U)		

DD FORM 1473
1 JAN 64

UNCLASSIFIED

Security Classification

UNCLASSIFIED
Security Classification

14. KEY WORDS	LINK A		LINK B		LINK C	
	ROLE	WT	ROLE	WT	ROLE	WT
Underwater explosions Nuclear Hydrodynamics						

INSTRUCTIONS

1. ORIGINATING ACTIVITY: Enter the name and address of the contractor, subcontractor, grantee, Department of Defense activity or other organization (corporate author) issuing the report.

2a. REPORT SECURITY CLASSIFICATION: Enter the overall security classification of the report. Indicate whether "Restricted Data" is included. Marking is to be in accordance with appropriate security regulations.

2b. GROUP: Automatic downgrading is specified in DoD Directive 5200.10 and Armed Forces Industrial Manual. Enter the group number. Also, when applicable, show that optional markings have been used for Group 3 and Group 4 as authorized.

3. REPORT TITLE: Enter the complete report title in all capital letters. Titles in all cases should be unclassified. If a meaningful title cannot be selected without classification, show title classification in all capitals in parenthesis immediately following the title.

4. DESCRIPTIVE NOTES: If appropriate, enter the type of report, e.g., interim, progress, summary, annual, or final. Give the inclusive dates when a specific reporting period is covered.

5. AUTHOR(S): Enter the name(s) of author(s) as shown on or in the report. Enter last name, first name, middle initial. If military, show rank and branch of service. The name of the principal author is an absolute minimum requirement.

6. REPORT DATE: Enter the date of the report as day, month, year, or month, year. If more than one date appears on the report, use date of publication.

7a. TOTAL NUMBER OF PAGES: The total page count should follow normal pagination procedures, i.e., enter the number of pages containing information.

7b. NUMBER OF REFERENCES: Enter the total number of references cited in the report.

8a. CONTRACT OR GRANT NUMBER: If appropriate, enter the applicable number of the contract or grant under which the report was written.

8b, 8c, & 8d. PROJECT NUMBER: Enter the appropriate military department identification, such as project number, subproject number, system numbers, task number, etc.

9a. ORIGINATOR'S REPORT NUMBER(S): Enter the official report number by which the document will be identified and controlled by the originating activity. This number must be unique to this report.

9b. OTHER REPORT NUMBER(S): If the report has been assigned any other report numbers (either by the originator or by the sponsor), also enter this number(s).

10. AVAILABILITY/LIMITATION NOTICES: Enter any limitations on further dissemination of the report, other than those

imposed by security classification, using standard statements such as:

- (1) "Qualified requesters may obtain copies of this report from DDC."
- (2) "Foreign announcement and dissemination of this report by DDC is not authorized."
- (3) "U. S. Government agencies may obtain copies of this report directly from DDC. Other qualified DDC users shall request through _____."
- (4) "U. S. military agencies may obtain copies of this report directly from DDC. Other qualified users shall request through _____."
- (5) "All distribution of this report is controlled. Qualified DDC users shall request through _____."

If the report has been furnished to the Office of Technical Services, Department of Commerce, for sale to the public, indicate this fact and enter the price, if known.

11. SUPPLEMENTARY NOTES: Use for additional explanatory notes.

12. SPONSORING MILITARY ACTIVITY: Enter the name of the departmental project office or laboratory sponsoring (paying for) the research and development. Include address.

13. ABSTRACT: Enter an abstract giving a brief and factual summary of the document indicative of the report, even though it may also appear elsewhere in the body of the technical report. If additional space is required, a continuation sheet shall be attached.

It is highly desirable that the abstract of classified reports be unclassified. Each paragraph of the abstract shall end with an indication of the military security classification of the information in the paragraph, represented as (TS), (S), (C), or (U).

There is no limitation on the length of the abstract. However, the suggested length is from 150 to 225 words.

14. KEY WORDS: Key words are technically meaningful terms or short phrases that characterize a report and may be used as index entries for cataloging the report. Key words must be selected so that no security classification is required. Identifiers, such as equipment model designation, trade name, military project code name, geographic location, may be used as key words but will be followed by an indication of technical context. The assignment of links, roles, and weights is optional.

DD FORM 1473 (BACK)
1 JAN 64

UNCLASSIFIED
Security Classification

SUPPLEMENTARY

INFORMATION



DEPARTMENT OF THE NAVY

OFFICE OF NAVAL RESEARCH
800 NORTH QUINCY STREET
ARLINGTON, VA 22217-5660

IN REPLY REFER TO

5510/1
Ser 931/412
5 May 94

From: Chief of Naval Research
To: Chief of Naval Operations (N312J)

Subj: DOCUMENT DECLASSIFICATION

ERRATA

Ref: (a) CNO ltr Ser 4U623674 of 2 May 94

Encl: (1) Copy of report "Hydra IIB Series - Transfer and Distribution of Traced Explosion Products to the Columns of Shallow Underwater Explosions" dtd 30 September 1965 (AD 370 910L)

1. In response to reference (a), enclosure (1) has been reviewed for declassification. Enclosure (1) has been downgraded to UNCLASSIFIED, appropriately marked, and is returned for your use. Distribution Statement A has been applied to enclosure (1).

2. If you have any questions, please call me on (703) 696-4619.

ERRATA - AD 370 910L


PEGGY LAMBERT
By direction

→ Copy to:
DTIC-OCD (William B. Bush)

151.2018